Interaction of Na^+, K^+, Mg^{2+} and Ca^{2+} Counter Cations with RNA

Stefan K. Kolev[1], Petko St. Petkov[2], Miroslav A. Rangelov[3], Dimitar V. Trifonov[4], Teodor I. Milenov[1], Georgi N. Vayssilov[2*]

[1] *Institute of Electronics, Bulgarian Academy of Sciences, 72 Tzarigradsko Chaussee Blvd., 1784 Sofia, Bulgaria*

[2] *Faculty of Chemistry and Pharmacy, University of Sofia, Boulevard James Bouchier 1, 1126 Sofia, Bulgaria, e–mail: gnv@chem.uni–sofia.bg*

[3] *Laboratory of BioCatalysis, Institute of Organic Chemistry, Bulgarian Academy of Sciences, Str. Acad. G. Bontchev, Bl. 9, 1113 Sofia, Bulgaria*

[4] *BioDiscovery, Pensoft, Prof. Georgi Zlatarski Street 12, 1700 Sofia, Bulgaria*

Abstract

Alkaline and alkaline earth ions, namely Na^+, K^+, Mg^{2+} and Ca^{2+}, are critical for the stability, proper folding and functioning of RNA. Moreover, those metal ions help to facilitate macromolecular interactions as well as the formation of supramolecular structures (e.g. the ribosome and the ribozymes). Therefore, identifying the interactions between ions and nucleic acids is a key to the better comprehension of the physical nature and biological functions of those biomolecules. The scope of this review is to highlight the preferential location and binding sites of alkaline and alkaline earth metal ions compensating the negatively charged backbone of nucleic acids and interacting with other electronegative centers, focusing on RNA. We summarize experimental studies from X-ray crystallography and spectroscopic analysis (infrared, Raman and NMR spectroscopies). Computational results obtained with classical and *ab initio* methods are presented afterwards.

Keywords: RNA, ribosome, Na^+, K^+, Mg^{2+} and Ca^{2+}

1 Introduction

The scope of this review is to highlight the preferential location and binding sites of Na^+, K^+, Mg^{2+} and Ca^{2+} metal ions compensating the negatively charged backbone of nucleic acids (NA) and interacting with other electronegative centers in those molecules, focusing on RNA. Metal ions are necessary to neutralize the negatively charged phosphate groups in the NA backbone. Na^+, K^+, Mg^{2+} and Ca^{2+} are exactly the counter cations, that play a key role in maintaining the stability, proper folding and functioning of nucleic acids[1-3]. Thus, Na^+, K^+, Mg^{2+} and Ca^{2+} were chosen for the review because of their biological importance. The ions carrying single positive charge, Na^+, K^+, form the ionic atmosphere around nucleic acids[4]. On the other hand, divalent ions, Mg^{2+}, Ca^{2+}, can bind to specific parts of the NA backbone, thus stabilizing the secondary and tertiary structure[5]. The presence of metal ions is required so that the structural integrity of chromosomes in various living cells (including mammalian cells) is preserved[6,7]. These ions ensure proper folding of the chromosomal DNA. In addition to neutralizing the negative charge of the backbone and maintaining the spatial form of DNA and RNA, metal ions act as mediators of the interaction between different macromolecules and formation of supramolecular structures[5, 8-10]. A typical example is the stabilization of the whole ribosome, containing both RNA and proteins[11-16]. Another example is the participation of Mg^{2+} for inducing conformational changes at the internal ribosome entry site of the hepatitis C virus[17]. Some metal ions can as well be used as dopants capable of changing the electro-chemical and physical properties of NA in order to produce new materials with applications in electronics and photonics[18].

Interactions between metal ions and various DNA or RNA sequences have been investigated by various experimental techniques. The centers, where mono- and divalent ions bind to macromolecules, have been characterized in solution as well as in crystal phase by NMR spectroscopy[8, 9, 19-21]. Vibrational techniques have been used as well, including infrared (IR) spectroscopy[22, 23] and Raman spectroscopy[24-29]. The interactions between the ions and phosphate group have been analyzed via the symmetric and asymmetric vibrations of the later. Model esters of the phosphoric acid with alcohols were used to help assign the phosphate vibrations[30-32]. Also, low frequency vibrations were found to be indicative for the presence of alkali metal ions near the phosphate groups of DNA[33].

The locations of the metal ions in crystal phase can be determined by X-ray crystallography[8, 9, 11, 12, 34-38]. However, it is often difficult to determine exact positions due to irregular distribution of the ions. A specific problem is distinguishing Na^+ ion from the water molecules[8]. Another complication in the interpretation of the results is the different structure of biomolecules in the crystal form and in solution. Experimental data derived from solution based systems at physiological conditions are more relevant for biological systems, but the techniques used in these studies (NMR, EPR, vibration spectroscopies) give only indirect information

about the metal ion – nucleic acid interactions. In most cases these techniques can yield only qualitative results.

The structure and processes taking place in the studied systems, derived from the experimental techniques, may be complemented by simulations, based on different theoretical methods. Commonly used theoretical approaches for simulation of the dynamics of biomolecules such as proteins, DNA or RNA are classical molecule dynamics (MD)[39-41] and Monte Carlo (MC) methods[42]. As the classic methods for MD simulations are parameterized for strictly defined systems, they can yield precise results if the parameterization is appropriate for the studied system[43]. In particular, the description of the local interactions of the metal ions with nucleic acid backbone within these methods strongly depends on the force field parameters. On the other hand, those interactions can be described adequately by simulations based on quantum chemical methods as most often density functional theory approach is used. Properly selected methods of first-principles quantum chemistry can precisely describe all types of interactions between atoms, ions, molecules or functional groups in the system, including electrostatic interactions, electron transfer and transitions, mutual polarization, Pauli repulsion. In addition to direct simulations of relevant systems, quantum chemical methods are used to parameterize potentials for the specific interactions employed in the classic MD or MC simulations[44]. A more detailed evaluation of the advantages, disadvantages and applications of classical and quantum mechanics as well as hybrid quantum mechanics – molecular mechanics methods for simulating the structure and properties of RNA can be found in the work of Ditzler *et al.* [45].

The application of quantum chemical methods can be done by structural optimization or *ab initio* dynamical simulations of biomolecule's fragments of interest. Examples of the optimization approach are studies of RNA fragments, containing Na^+ or Mg^{2+} ions. The water phase is usually modeled as a continuum solvent[46]. Quantum mechanical/molecular mechanical (QM/MM) methods can also be applied[45, 47]. By performing cluster model, non-periodic simulations with implicit solvation, it has been determined that Na^+ and Mg^{2+} ions have binding affinity to the phosphate groups of RNA. The affinity of Mg^{2+} is higher than that of Na^+ [46]. The other approach, *ab initio* molecular dynamic simulations, has been successfully used to determine the behavior of metal ions in various systems. Such systems include carbonates, or Na^+ and Mg^{2+} cations with RNA, studied in aqueous solutions[48, 49].

In the present review, we summarize results for RNA, based on experimental studies from X-ray crystallography and spectroscopic analysis (infrared, Raman and NMR spectroscopies). Computational results obtained with classical and *ab initio* methods are presented afterwards. In some parts of the review structures of DNA are also discussed.

2. Investigation of metal ions in nucleic acids by X-ray crystallography

2.1. Studies of short RNA sequences

The location of alkaline (Na^+ and K^+) and alkaline earth (Mg^{2+} and Ca^{2+}) ions in RNA or DNA molecules can be determined by X-ray crystallographic analysis with a relatively good spatial resolution, around 200 pm. High resolution has been achieved with small RNA/DNA sequences (less than 100 nucleotides)[50-52]. RNA fragments from viral[35, 53-55] or bacterial origin[36, 56, 57] have been used in the X-ray crystallographic studies. However, human RNA has also been utilized[58]. One should note that the structures of biomolecules in the living cells differ from those obtained from crystallographic images. The XRD results represent a single picture in time, without dynamical changes, while in the living cells biomolecules and ions interact dynamically in order to carry out their functions. Moreover, solid state RNA and DNA molecules have restricted conformational freedom compared to aqueous solution. The results are also affected by the low temperature, 100-120^{o}K, at which the XRD measurements are performed[37].

Tables 1 to 4 contain X-ray crystallographic data of the corresponding metal ions, interacting with RNA molecules (less than 100 nucleotides). Only structures with a resolution better than 200 pm are selected. Those examples of short sequences, because their aim is to present the first coordination shell of the ions, with maximal resolution and precision. High resolution is difficult to be achieved in larger amorphous systems, like the whole ribosomal subunits[11]. Thus, the chosen structures are either parts of larger biomolecules, or short synthetic sequences[34-36, 50-60]. Molecules classified as small RNAs have not been included[61]. The files with the corresponding PDB codes can be found in the Protein Data Bank (http://www.rcsb.org).

Table 1. Examples of atoms, which are in direct contact with selected Mg^{2+} ions and form their first coordination shell. All listed results are obtained from X-ray crystallographic data for RNA molecules, the corresponding reference is shown in parentheses. The distances are given in pm.

PDB code	**Ion #**	**R(Mg-O) or R(Mg-N)**		
Resolution		**H_2O**	**PO_4^-**	**Others**
2OE5/150[58]	Mg 103	212, 225, 202, 217, 200, 200		
human ribosomal decoding site	Mg 104	216, 221, 192, 218, 216, 193		
1F27/130[51]	Mg 34	221, 209, 199, 204, 246, 204, 219		Mg 39-288
synthetic biotin-binding pseudoknot	Mg 35	204, 209, 208		O4U-231
	Mg 36	203, 216, 212, 206, 216	201	
	Mg 37	230, 224, 207, 197, 197	192	

	Mg 39	202, 225, 196, 196, 211, 213, 307		Mg 34-288
2A43/134[54]	Mg 201	209, 213, 227, 230, 224		O6G-237
luteoviral RNA pseudoknot	Mg 207	216, 218, 210, 209, 210, 219, 312		
354D/150[36]	Mg 200	219, 212, 229, 197, 226, 190		
loop E from *Escherichia coli* 5S ribosomal RNA	Mg 201	227, 247, 221, 181, 214	205	Mg 202-270
	Mg 202	241, 220, 188, 211, 268	214	Mg 201-270
	Mg 203	208, 216, 194, 232, 239, 221		
	Mg 204	227, 227, 222, 235, 201		O6G-260

Table 1 shows data from PDB files of various structures containing Mg^{2+} ions forming complexes with RNA molecules. The chosen structures include the loop E from *Escherichia coli* 5S ribosomal RNA[36]; synthetic biotin-binding pseudoknot[51]; luteoviral RNA pseudoknot[54], and human ribosomal decoding site fragment[58]. Zheng *et al*. identified seven Mg^{2+}-binding motifs in RNA crystal structures: a Y-clamp motif (Figure 1A); a U-phosphate motif (Figure 1B); a 12-member ring motif (Figure 1C); a purine N7-seat motif (Figure 1D); G-N7 macrochelates I and II motifs (Figure 1E,F)[62]. A 10-member ring with purine N7 motif has also been observed, Figure 1G.

Due to its strong electrostatic field, the divalent magnesium cation has high affinity toward electronegative atoms and groups. The most frequent coordination number of Mg^{2+} is 6 (Table 1, Figure 1), which corresponds to 6 electronegative centers, arranged octahedrally. Such centers include the oxygen atoms of water molecules, denoted below as $O(H_2O)$, and O atoms of phosphate groups, belonging to nucleic acid backbone. Nitrogen or oxygen atoms of the nucleobases are included in the coordination shells of Mg^{2+} ions in rare cases. The Mg^{2+}-$O(H_2O)$ distances vary between 181 and 268 pm for double-stranded RNA complexes (Table 1). The average Mg^{2+}-$O(H_2O)$ distance, observed in Mg^{2+} complexes with DNA is 207.5 pm. This value is determined for structures composed of double-stranded DNA, consisting of less than 100 nucleotides[37]. When Mg^{2+} ions are directly bonded to an oxygen atom of the phosphate groups in the Mg^{2+}-RNA complex, the corresponding Mg^{2+}-O is in the range of 200–215 pm. The average distance between the Mg^{2+} ion and PO_4^- group in DNA complexes is about 203 pm[37].

A typical example of magnesium ion, directly bonded to a phosphate group is Mg^{2+} 201 from PDB 354D, with Mg^{2+}-$O(PO_4^-)$ distance of 205 pm (Figure 2A). Magnesium ions can also make contacts with the PO_4^- groups through water molecules, like Mg^{2+} 200 from PDB 354D (Figure 2B). An example of the rare case, where the Mg^{2+} ion is coordinated to the electronegative centers of nucleobases, is Mg^{2+} 201 ion from PDB 2A43 (Figure 2C). The Mg^{2+}

201 ion is directly bonded to the O6 oxygen atom of guanine with Mg^{2+}-O6G distance of 237 pm[54]. Another example is Mg^{2+} 204 from PDB 354D, where the Mg^{2+}-O6G distance is 260 pm[36]. The oxygen atom O4 of uracil can also act as a ligand for the coordination of Mg^{2+} ions, as the Mg^{2+} 35 from PDB 1F27 with Mg^{2+}-O4U distance of 231 pm[51]. The Mg^{2+} ions can also be coordinated to the N7 nitrogen atoms of guanine with Mg^{2+}-N7G distances of 233 pm as reported for Mg^{2+}-DNA complexes[37].

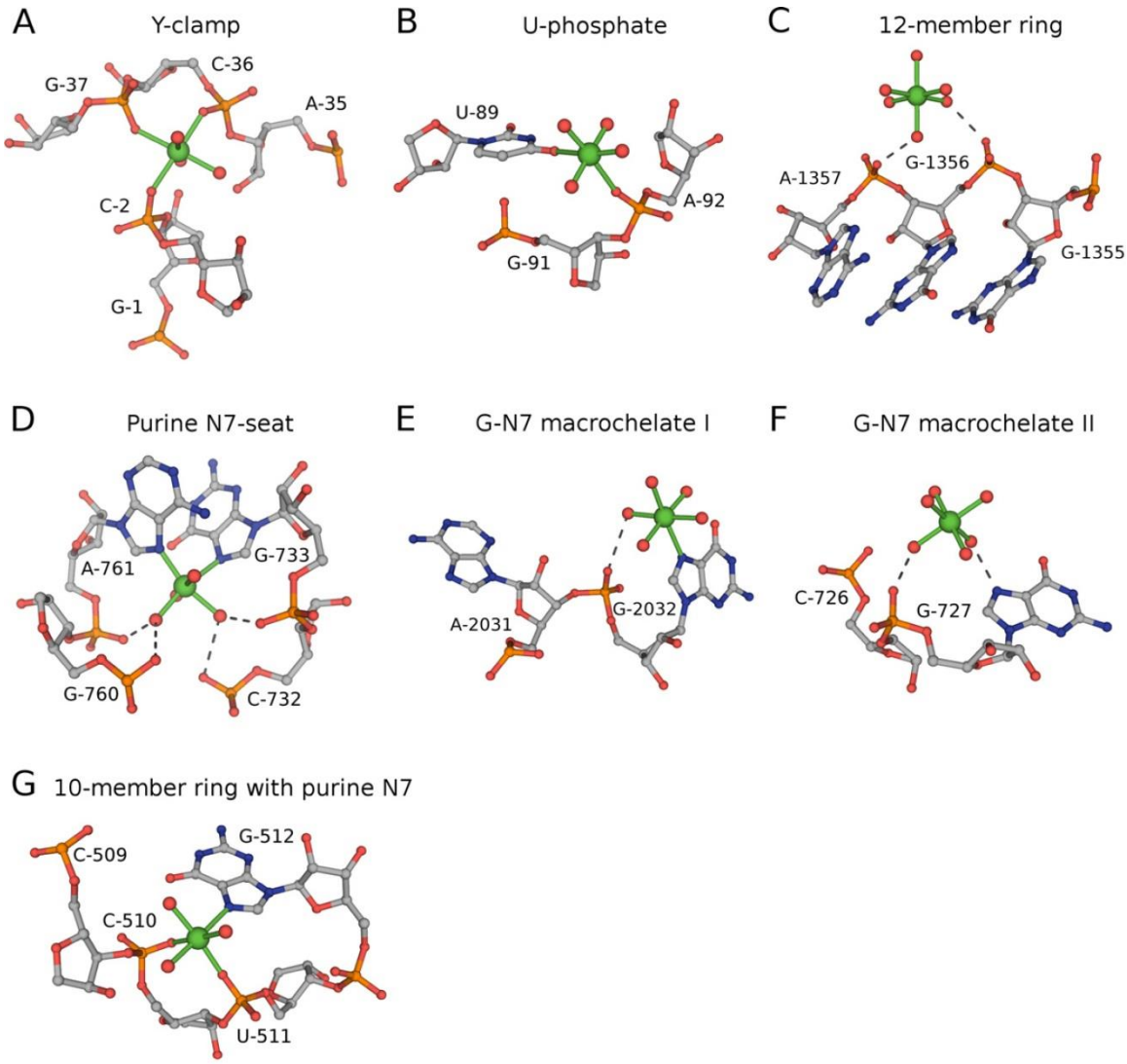

Figure 1. Magnesium-binding architectures (motifs) in RNA crystal structures as reported by Zheng *et al.*[58]. Mg^{2+} ions are shown in green. Hydrogen bonds are shown as gray dashed lines. The motif-forming nucleotides are labeled. (Reprinted from Ref. 58 under Creative Commons CC BY License, Copyright 2015 Oxford University Press).

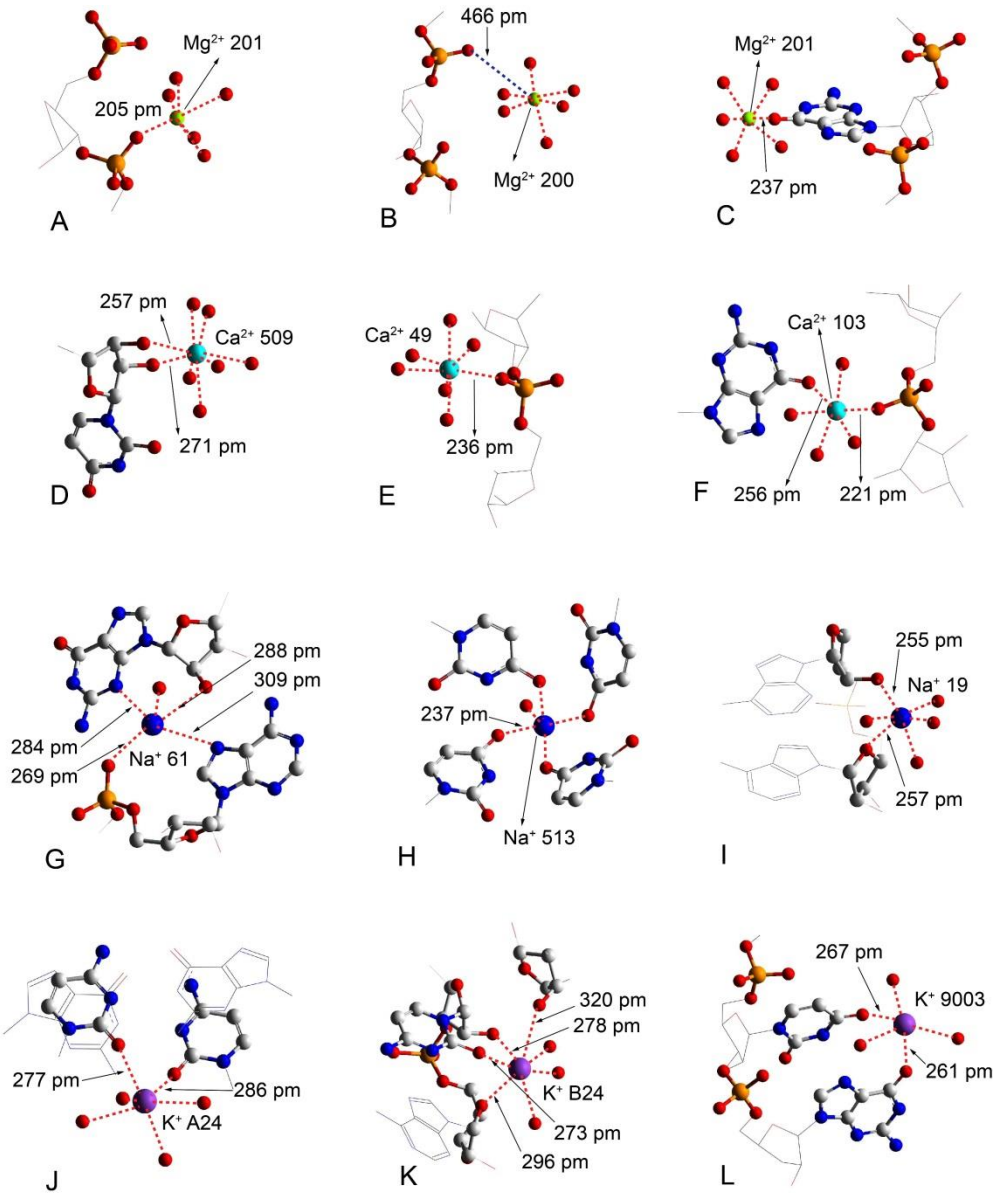

Figure 2. Sketches of specific ways of interaction of metal ions with RNA molecules based on data from PDB structures: A, B, C – with Mg^{2+} ions. Respective structure sources: PDB 354D (A and B)[36] and 2A43[54]; D, E, F – with Ca^{2+} ions. Respective structure sources: PDB 1J8G[52], 397D[53] and 2ZY6[50]; G, H, I – with Na^{+} ions. Respective structure sources: PDB 1L2X[35], 1J8G[52] and 3ND3[59]; J, K, L – with K^{+} ions. Respective structure sources: PDB 2OIY (J and K)[34] and 2QEK[60].

Crystallographic data for the complexes of Ca^{2+} is presented in Table 2. The chosen RNA structures, interacting with the ions, include: modified transfer RNA fragment TPHE39A[50]; RNA tetraplex (UGGGGU)(4)[52] and *HIV-1* trans-activation region RNA fragment[53]. The first coordination shell of Ca^{2+} ions is composed of 6 to 8 electronegative centers (Table 2, Figure 2D,E,F), most often oxygen atoms from water molecules. The Ca^{2+}–$O(H_2O)$ distance is in the range of 217-280 pm (Table 2). Ca^{2+} ions also have an affinity to the

oxygen atoms of the phosphate groups with Ca^{2+}-O(PO_4^-) with distances being in the rage of 221-253 pm (Table 2). They can bind to more than one phosphate group as well. Thus, a Ca^{2+} ion can stabilize the loop formation in a single strand of RNA by directly interaction with three phosphate groups (Figure 3), resulting in folding of the molecule[53].

Table 2. Examples of atoms, which are in direct contact with selected Ca^{2+} ions and form their first coordination shell. All listed results are obtained from X-ray crystallographic data for RNA molecules, the corresponding reference is shown in parentheses. The distances are given in pm. O2` and O3` denote corresponding oxygen atoms in the ribose moiety.

PDB code	**Ion #**	**R(Ca-O)**		
Resolution		**H_2O**	**PO_4^-**	**Others**
397D/130[53]	Ca 48	242, 236, 237	232, 228, 232	
HIV-1 trans-activation region RNA fragment	Ca 49	241, 246, 242, 233, 236, 248	236	
	Ca 50	238, 249, 234, 244, 237, 244	232	
	Ca 51	251, 266, 247, 217, 247, 242, 241, 242		
1J8G/61[52]	Ca 509	245, 255, 255, 257, 261, 252		O2`-271, O3`-257
RNA tetraplex (UGGGGU)(4)	Ca 510	260, 271, 268, 256, 253, 258	253	O4U-255
	Ca 511	260, 269, 280, 218		O2`-276, O3`-276
2ZY6/175[50]	Ca 102	238, 243, 235, 237, 235	231	
modified transfer RNA fragment TPHE39A	Ca 103	239, 247, 230, 242	221	O6G-256
	Ca 104	242, 252, 240, 250, 242, 243, 253		
	Ca 105	225, 230, 267, 220, 248, 252		O4U-258
	Ca 106	241, 228, 255	228, 232	O2C-231
	Ca 107	239, 230, 236, 249, 270		
	Ca 108	236, 223, 246		O6G-237

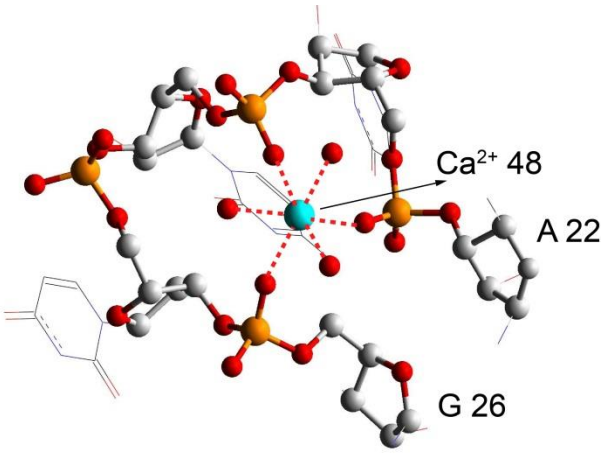

Figure 3. Folding of the RNA strand stabilized by the direct interaction of the Ca^{2+} ion with oxygen centers of three phosphate groups. Respective structure source: PBD 397D[53].

Apart from neutralizing the negatively charged phosphate groups of the RNA backbone, the Ca^{2+} ions also show an affinity to the oxygen atoms O2' and O3' of the ribose moiety. Measured distances between the ions and those centers are in the range of 257-276 pm[52]. In some crystals of Ca^{2+}-RNA complexes, direct contacts between the calcium cation and nucleobases have been observed: Ca^{2+}-O6G (with oxygen atoms of guanine) with lengths of 256 pm and 237 pm, or with O4 oxygen atoms of uracil with lengths of 255 pm and 258 pm[50, 52].

Crystallographic data for the complexes of Na^+ is presented in Table 3. The chosen RNA structures, interacting with the ions, include RNA pseudoknot from beet western yellow virus[35]; RNA heptamer double helix (*Escherichia coli* transfer RNA fragment)[56]; modified transfer RNA fragments from *Escherichia coli*[57] and 16-mer double-stranded RNA fragments (precursor messenger RNA from *Trypanosoma brucei*)[59]. The monovalent ions have affinity mainly to water molecules and RNA nucleobases, as presented in Tables 3 and 4. Na^+ ions have between four and six ligands. The Na^+-O(H_2O) distances are in the range of 210-270 pm, as exceptional cases some longer distances are reported (Table 3, Figure 2G,H,I).

Table 3. Examples of atoms, which are in direct contact with selected Na^+ ions and form their first coordination shell. All listed results are obtained from X-ray crystallographic data for RNA molecules, the corresponding reference is shown in parentheses. The distances are given in pm. O2` and O4` denote corresponding oxygen atoms in the ribose moiety.

PDB code	**Ion #**	**R(Na-O) or R(Na-N)**		
Resolution		**H_2O**	**PO_4^-**	**Others**

434D/116[57]	Na 8	255, 222, 223, 296, 294		
435D/140[57]	Na 1	241, 210, 241, 224		
	Na 8	222, 211		
466D/116[56]	Na 102	231, 231, 220, 220, 276, 276,		
3ND3/137[59]	Na 19	225, 228, 228, 233		O2`-255, O4`-257
1J8G/61[52]	Na 512			O4U–235, 235, 235, 235
	Na 513	240		O4U–237, 237, 237, 237
1L2X/125[35]	Na 61	267	269	O2`-288, N3G-284, N7A-309
	Na 62	277	274	O2`-271, O2C- 274
	Na 63	293	265	O2`-259, O4`-305
3ND4/152[59]	Na 19	224, 239, 256, 262, 216		N7A-264

In some complexes of Na^+ ions with RNA molecules sodium ion is coordinated to the phosphate group of the backbone with Na^+-O(PO_4^-) distance is in the range of 265–275 pm[35]. The same Na^+ ions are coordinated to O2' and O4' oxygen atoms of ribose and/or a center from a nucleobases. In the reported structures the measured Na^+-O2' distances range between 255 pm and 288 pm[35, 59]. Na^+-O4' distances of 257 pm and 305 pm are reported[35, 59]. Sodium can stabilize quadruple-stranded structures (Figure 2H), where the Na^+ ion is directly bonded to four carbonyl oxygen atoms, O4U, from four uracil nucleobases (PDB 1J8G with resolution of 61 pm). Na^+-O4U distances of 235 and 237 pm are measured in such structures[52]. Sodium ions have affinity to the other nucleobases as well, and bind directly to their electronegative centers. For example, Na^+ 19 from PDB 3ND4 binds directly to the N7 nitrogen atom of adenine (Na^+-N7A distance is 264 pm)[59].

Table 4. Examples of atoms, which are in direct contact with selected K^+ ions and form their first coordination shell. All listed results are obtained from X-ray crystallographic data for RNA molecules, the corresponding reference is shown in parentheses. The distances are given in pm. O2`, O3' and O4` denote corresponding oxygen atoms in the ribose moiety.

PDB code	**Ion #**	**R(K-O)**		
Resolution		**H_2O**	**PO_4^-**	**Others**
2QEK/180[60]	K 9001	275, 274		O4U-275, O6G-273

	K 9002	288	O4U-283, O6G-275
	K 9003	282, 268, 307	O4U-267, O6G-261
3C44/200[60]	K A 25	285	O4`-295
	K B 25	274	O4U-268, O6G-266
	K B 28	291	O2`-298, O3`-303
2OIY/160[34]	K A 24	302, 288, 321, 305	O2C-277, 286
	K B 24	296, 251, 277	O2`-278, 320, O2C-273, O4`-296
	K A 25	292, 305, 308, 321	O6G-305, 291, O4U-278
1ZCI/165[55]	K A 24	260, 274, 272, 271	O6G-270, O4U-262
	K B 24	286, 268, 290, 261	O6G-265, O4U-258
	K C 24	261, 276, 312, 272	O6G-274, O4U-264
	K D 24	263, 270, 265, 270	O6G-271, O4U-261

Dimerization initiation site *HIV-1* RNA fragments are chosen as examples of K^+-RNA crystalline complexes, Table 4[34, 55, 60]. K^+ ions usually coordinate 5-7 electronegative centers, Figure 2J,K,L. In some potassium positions, however, some of the coordinated water molecules were not detected with X-ray crystallography (see RDB 2QEK and 34CC, Table 4). The K^+-O(H_2O) distance is in the range of 251-321 pm (Table 4). The K^+-O2' distance to the oxygen atom O2' of ribose is in the range of 280–320 pm, see PDB 3C44 and 2OIY[34, 60]. Furthermore, K^+ ions can be in direct contact with the O4 oxygen atoms of uracil or O6 oxygen atoms of guanine, with K^+-O distances of 261–283 pm and 261–305 pm, respectively.

2.2. Transfer RNA

The transfer RNA (tRNA) function is to deliver specific amino acids to the peptidyl transferase region in the ribosome according to the messenger RNA (mRNA) sequence[63]. Moreover, tRNA takes part in the catalysis during the peptide biosynthesis. The tRNA molecule is flexible and capable of forming double-stranded regions as well as loops (Figure 4). The anticodon loop contains 7 nucleotides, including 34, 35 and 36. The anticodon binds to the specific trinucleotide code of the mRNA, which assures the proper sequence of amino acids during the synthesis of the polypeptide chain. The amino acid binds to the amino acid-attachment site of tRNA via the process of aminoacylation, which is aided by the enzyme aminoacyl tRNA synthetase. It is the 2'-OH group of the 3' end of the aminoacylated tRNA that takes part in the catalysis during the peptide biosynthesis[64, 65].

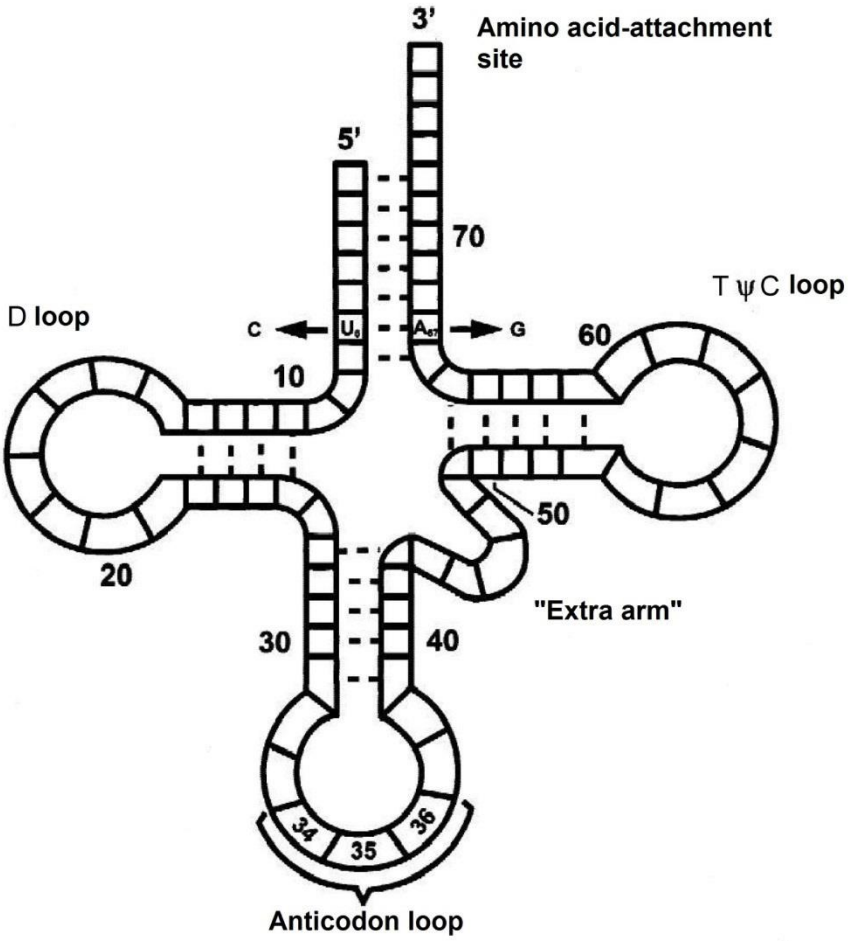

Figure 4. Secondary structure of phenylalanine tRNA derived from yeast according to reference[70]. The double-stranded regions as well as the D-loop (nucleotides 13-22), TψC loop (nucleotides 53-61), anticodon (nucleotides 34-36), and the 3' end, which binds to the amino acid, are shown here. (Reprinted from Ref. 70 under Creative Commons License Attribution NonCommercial 4.0 International License, 2000, Publisher: Cold Spring Harbor Lab Press).

The divalent cations are found critical for preservation the structural stability of tRNA. The X-ray crystallographic studies have shown that Mg^{2+} ions bind directly to the phosphate groups or nucleobases of the nucleotides of tRNA as well as via water molecules, see PDB files 4TNA, 1TRA, 2TRA, 4TRA, 6TNA and 1EHZ[66-70]. Table 5 shows data from PDB files (PDB 1EHZ; 2TRA of the various structures containing Mg^{2+} ions forming complexes with tRNA molecules. The crystallographic study of Shi *et al*. on phenylalanine tRNA (PDB 1EHZ), which has good resolution - 193 pm, is chosen for analyzing the interaction Mg^{2+}-tRNA (see PDB 1EHZ Table 5). Figure 5 illustrates the most complex region of phenylalanine tRNA regarding the interactions with magnesium cations. Mg^{2+} 560 is fully hydrated with 6 molecules of water and is located in the center of a cycle formed of nucleotides 7-13. The ions Mg^{2+} 580 and Mn^{2+} 550 form a two center complex which interacts with the tRNA between the amino acid-attachment site and the D-loop. The ion Mn^{2+} 550 is directly bonded to the N7G nitrogen atom

of guanine from nucleotide G15, while Mg^{2+} 580 is bonded to the phosphate groups of nucleotides U7 and A14. In Figure 5, only four of all six ligands of Mg^{2+} 580 are shown – two oxygen centers from the phosphate groups and two oxygen atoms from water molecules. The oxygen atoms from the other two water molecules are omitted for clarity. The location of the metal ions between two phosphate groups stabilize the folding of the tRNA by bridging the negatively charged phosphate groups, thus transforming electrostatic repulsion between them into electrostatic attraction to the magnesium ions.

Table 5. Examples of atoms which are in direct contact with selected Mg^{2+} ions and form their first coordination shell. All listed results are obtained from X-ray crystallographic data for RNA molecules, the corresponding reference is shown in parentheses. The distances are given in pm.

PDB code	**Ion #**	**R(Mg-O) or R(Mg-N)**		
Resolution		**H_2O**	**PO_4^-**	**Other**
1EHZ/193[70]	Mg 510	200, 200, 200, 200, 201		
	Mg 540	200, 200, 200	207, 211	
	Mg 560	200, 200, 200, 200, 200, 201		
	Mg 570	200, 200, 200, 200, 200, 201		
	Mg 580	200, 278, 323	193, 261	
	Mg 590		253	N6A-300, N7A-309
	Mn 520	200, 200, 200, 200, 200		N7G-230
	Mn 530	200, 200, 201, 201	219	O2'-234
	Mn 550	200, 200, 200, 200, 201		N7G-248
2TRA/300[67]	Mg 77	199, 199, 199, 198, 198, 197		

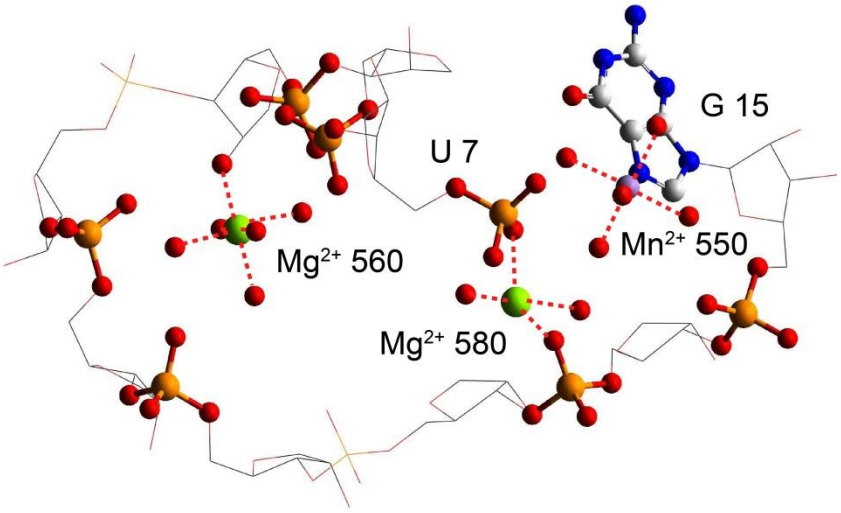

Figure 5. An outline of tRNA from uracil 7 to guanine 15 stabilized by the metal ions Mg^{2+} 560, Mg^{2+} 580 and Mn^{2+} 550. Respective structure source: PDB 1EHZ.

2.3. Ribosomal RNA

Metal ions are necessary also for the proper structure and the protein biosynthesis function of ribosomes in the living cells. Typical concentration of alkaline and alkaline-earth cations in the cytosol (for mammalian cells) are 139 mM L^{-1} for K^+; 12 mM L^{-1} for Na^+; 0.8 mM L^{-1} for Mg^{2+}; and <0.0002 mM L^{-1} for Ca^{2+} [63]. This relatively high concentration of K^+ ions in the cytosol is connected with their role in the proper functioning of the ribosomal RNA (rRNA). K^+ ions are needed, in order to provide nonspecific charge neutralization of the rRNA phosphate backbone. Potassium ions can also bind to specific sites of the rRNA, thus stabilizing the tertiary structure[71, 72].

The structure and functioning of the ribosomes also depend on the presence of Mg^{2+} ions. For example, Mg^{2+} ions contribute to the coupling of the small and large ribosomal subunits in the living cells[73-75]. Pioneering studies of McCarthy had shown that cultivation of *Escherichia coli* in the absence of Mg^{2+} ions leads to a decrease in the number of ribosomes in the bacterial cells[76]. This effect may be related to the participation of Mg^{2+} ions in the formation and preservation of the structural integrity of the ribosomes. Moreover, if the negative charges of the RNA phosphate groups are compensated by protonated polyamines, instead of metal ions, the large ribosomal subunit of *E. coli* irreversibly loses its quaternary structure. The peptidyl transferase activity is lost too[77, 78]. The processes of polynucleotides coupling in the ribosome, as well as the attachment of the ribosome to the endoplasmic reticulum, are found to be dependent on the presence of Mg^{2+} ions[79, 80].

Magnesium ions are part of the peptidyl transferase domain, where they coordinate to phosphate groups or ribose, without taking part in the protein biosynthesis[13-16].

The importance of K^+ ions to the functionality of mammalian ribosomes is deducible by the loss of peptidyl transferase activity and spatial structure, when they are placed in an environment without K^+ ions[81]. On the other hand, the ribosomes of *E. coli* decompose into the individual subunits when they are exposed to high concentrations of K^+ ions[82]. Apparently, this is due to the competitive binding of K^+ ions to the centers, which accommodate Mg^{2+} in order to accomplish subunits coupling.

In order to analyze the interaction of ribosomal RNA with metal ions, an X-ray crystallographic study on the large subunit of *Haloarcula marismortui* has been performed. Resolution of 240 pm has been achieved (PDB 1S72)[11]. The investigated subunit contains 3045 nucleotides. Additionally, 31 proteins and 116 Mg^{2+} ions have been identified in it[83]. Part of the ions is completely solvated by water, while another part interacts directly with fragments of the ribosomal subunit.

Magnesium ions are classified into six types, from type 0 to type V, according to the number of the ligands from RNA or proteins, coordinated to them. Type 0 have zero ligands (Figure 6A), type I – one (Figure 6B), type II – two (Figure 6C,D), type III – three (Figure 6E,F), type IV - four, and type V – five. Six ligands have not been observed. Type I-III, presented in Figure 6, are the ion configurations most often observed[11]. Type II structures have been divided in two groups, according to the location of the bonded ligands. In group “a” - the ligands are located only on one side of the ion, Figure 6C. In group “b” – the ligands are located on the both sides, Figure 6D. In Mg^{2+} ions type IIIa, the inner-sphere ligands lie in a single plane that includes the metal ion, whereas in type IIIb, the inner-sphere ligands are mutually orthogonal, Figure 6E,F.

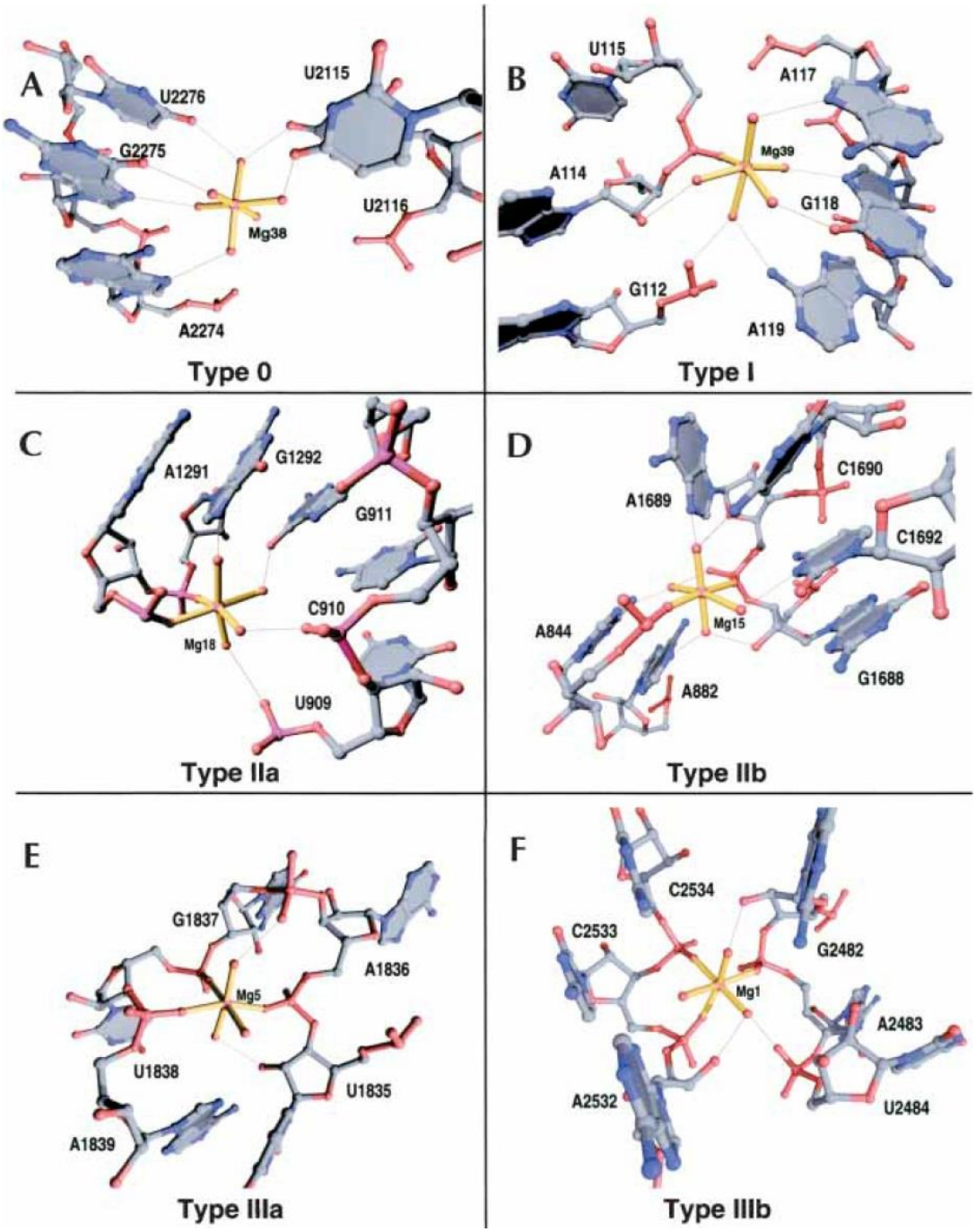

Figure 6. Examples of different types of coordination of Mg^{2+} ions, as observed in the large subunit of the *H. marismortui* ribosome[11]. The six bonds from the coordination shell of the Mg^{2+} ions are shown in yellow. (Reprinted from Ref. 11 under Creative Commons License Attribution NonCommercial 4.0 International License, 2004, Publisher: Cold Spring Harbor Lab Press).

The role of Mg^{2+} ions, presented in the large ribosomal subunit is to stabilize the structure of the 23S RNA. The Mg^{2+} from type IIa (40 ions, 34,5%) are most frequently observed, followed by the type I (37 ions, 31,9%). The Mg^{2+} ions of both types usually

neutralize regions of the secondary RNA structures with closely packed PO_4^- groups. Only nine type 0 ions are observed. The Mg^{2+} ions of types III, IV and V contribute to the remaining 17,2% of the total number of Mg^{2+} ions in the system, as only single Mg^{2+} ions belong to types IV and V. These ions, types III to V, are usually bonded to specific single-stranded structures such as loops etc. For the whole structure 200 direct contacts of the Mg^{2+} ions with ligands originating from RNA are counted. Direct Mg^{2+}-O(H_2O) contacts are 378. From all direct contacts of Mg^{2+} ions with RNA-originating ligands, those with oxygen atoms of phosphate groups are the most frequently observed: 73% of all direct contacts. The indirect interactions of the magnesium ion and phosphate group mediated via water molecules (Mg^{2+}-H_2O-PO_4^-) account for 50% of all indirect interactions.

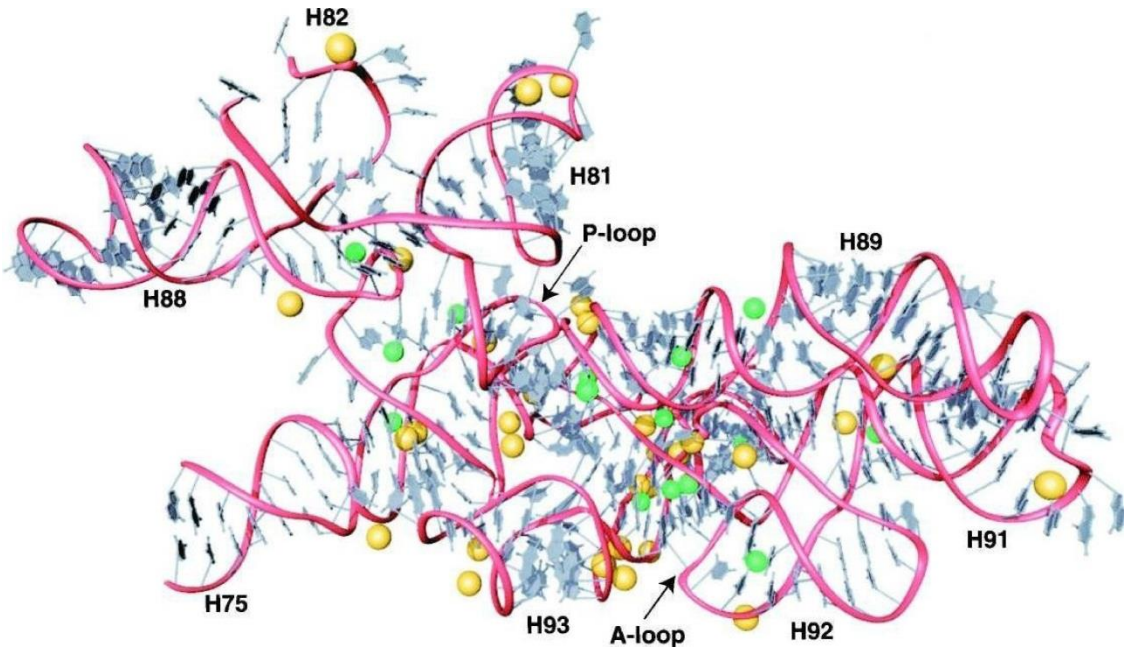

Figure 7. 3D representation of metal ion binding centers in the peptidyl transferase region. The RNA backbone is shown in red, the nucleobases are shown in grey, the Mg^{2+} ions and the monovalent cations are colored in yellow and in green, respectively. The nucleotides with numbers 2084-2127, 2266-2321 and 2419-2660 are shown in the figure (the numbering is according to the rRNA of *H. marismortui*)[11]. (Reprinted from Ref. 11 under Creative Commons License Attribution NonCommercial 4.0 International License, 2004, Publisher: Cold Spring Harbor Lab Press).

The indirect interactions, via water molecule, of Mg^{2+} ions with N7 atoms of adenine and guanine are substantially more frequent than the direct contacts, 63 and 11, respectively[11]. Mg^{2+} ions are also found in the groove regions of double-stranded RNA[84].

About half of the Mg^{2+} ions and one third of the Na^{+} ions, found in the large ribosomal subunit, are located within the peptidyl transferase region of domain V and the evolutionary preserved regions of domains II and IV[11]. The later regions are in direct contact with the peptidyl transferase center (Figure 7). Around 40% of all nucleotides in the central loop of domain V interact directly with Na^{+}, K^{+} or Mg^{2+} ions[11]. The double-helix region 90 (Helix 90) and the location, where it couples with the central loop, contain a large amount of metal ions stabilizing the structure. For example, the nucleotide G2618 is in direct contact with 3 Mg^{2+} ions, two of which are of type I, and the third one is of type II. The first two ions are bonded directly to the phosphate group of G2618. The third Mg^{2+} ion bridges the phosphate groups of nucleotides G2618 and G2617. Thus, metal ions, especially the Mg^{2+}, play a crucial role ensuring the stability of the peptidyl transferase region. However, metal ions do not take part in the peptide biosynthesis.

The monovalent cations Na^{+} and K^{+} do not have preferred coordination geometry. More specifically, 88 monovalent cations have been detected in the large ribosomal subunit of *H. Marismortui*[11]. They are classified in four groups according to their location and the electronegative centers to which they bind: (1) ions within the major groove in double-stranded RNA; (2) ions bonded to ribosomal proteins; (3) ions located in the space between the ribosomal proteins and RNA; and (4) ions bonded to specific electronegative centers. The most frequently observed contacts of the monovalent ions with 23S RNA are with the guanine nucleobases or stacked guanine and cytosine bases in the area of the major groove of the RNA. The cation usually interacts directly with O6 atoms of guanine or O4 atoms of uracil. The typical distance between the Na^{+} ions and the atoms from the RNA nucleaobases is between 280 and 320 pm.

Comparing the binding of the monovalent ions within the ribosome with that of the Mg^{2+} ions, one may conclude that the Mg^{2+} ions coordinate predominantly to the oxygen centers of the phosphate groups of the RNA backbone. The monovalent cations coordinate in most cases to the electronegative centers of nucleobases and ribosomal proteins. In the example discussed above, Na^{+} and K^{+} ions have in total 138 direct contacts to nucleobases and only 55 to phosphate groups[11].

3. Investigation of metal ions in nucleic acids via spectroscopic methods

In this part we will summarize the studies of the interaction of metal ions with nucleic acids using spectroscopic methods – vibrational spectroscopies, infrared and Raman, and NMR spectroscopy.

3.1. Vibrational spectroscopies

Most of the studies on the interaction of metal ions with RNA or DNA using vibrational spectroscopies, infrared (IR) and Raman, consider the shifts of the symmetric and

antisymmetric vibrations of the phosphate groups in nucleic acids as an indication for their interactions with metal ions. Simplified model compounds (like sodium diethyl phosphate and sodium dimethyl phosphate) are used for clarifying the trend in the frequency shifts of symmetric (ν_s) and antisymmetric (ν_{as}) vibrations of the esterified phosphate group[30, 31]. The vibrational spectra of the compounds have been studied in solution at neutral pH=7 for $Na^+Et_2PO_4^-$ and at pH=7.2 for $Na^+Me_2PO_4^-$ [30, 31]. For dimethyl phosphate, studied by Raman spectroscopy in solution (Figure 8, upper spectrum) the symmetric vibrations appear at 1083 cm^{-1}. The antisymmetric vibrations are observed at higher frequencies, 1217 cm^{-1} [31]. In the crystal phase (Figure 8, middle spectrum) both the symmetric and antisymmetric vibrations shift to higher frequencies, at 1125 cm^{-1} and 1245 cm^{-1}, respectively[31]. The intensity of the symmetric vibrations observed in Raman spectra is high, whereas that of antisymmetric vibrations is low.

In the IR spectrum of sodium diethyl phosphate (water solution), the symmetric vibrations have a medium intensity and appear at 1080 cm^{-1}, whereas the antisymmetric ones have high intensity and are observed at 1200 cm^{-1} [30].

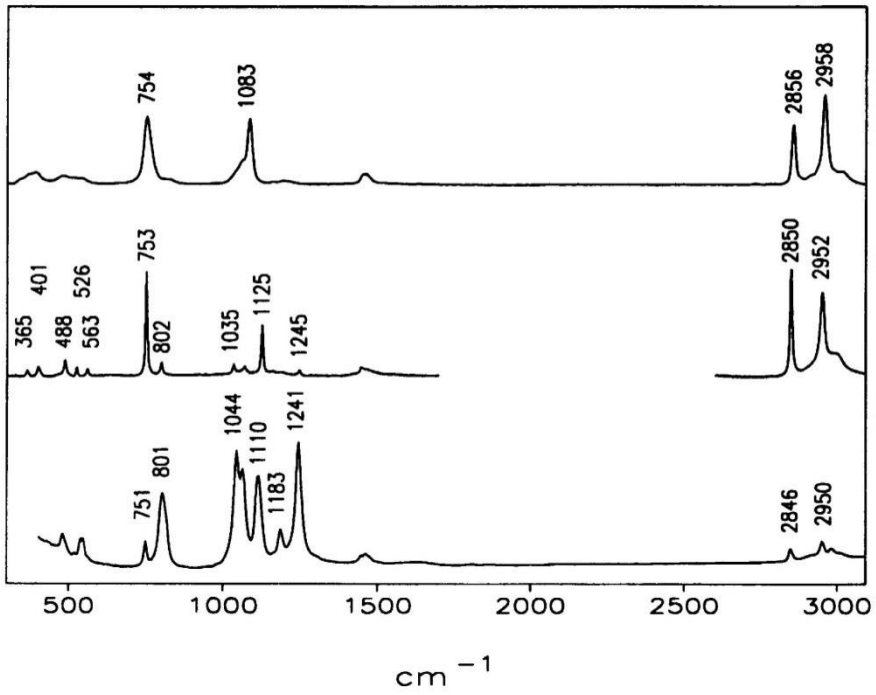

Figure 8. Vibration spectra of $Na^+(CH_3)_2PO_4^-$: upper spectrum – Raman spectrum in 0.8 M solution at pH=7.2, middle spectrum – Raman spectrum in polycrystalline solid phase, lower spectrum – infrared spectrum of the compound in KBr pellets[31]. (Reprinted from Ref. 31, Copyright 1994 with permission from Elsevier).

The spatial arrangements of DNA and RNA molecules differ because of the different tasks they perform. The RNA molecules form more complex tertiary and quaternary structures in order to accomplish their diverse functions: translation of genetic code into proteins, acting

as a messenger molecule, selective delivery of amino acids, catalyzing synthesis of the peptide bonds. DNA molecules, on the other hand, remain mostly in double-stranded form, in order to store genetic information[63]. Thus, the way of interaction between magnesium ions and DNA or RNA is expected to be different. Spatial effects make direct binding of Mg^{2+} ions to RNA more probable, than binding to DNA. Vibrational spectroscopy studies illustrate this different behavior of Mg^{2+} ions, towards the nucleic acids[24, 27].

By using Raman spectroscopy, the influence of Mg^{2+} ions on the vibration frequencies of the phosphate groups of DNA in solution has been studied[24, 26]. The measured frequency of symmetric vibrations of the phosphate groups in absence of metal ions is 1093 cm^{-1} [26] or 1079 cm^{-1} [24]. The frequency is slightly downshifted by adding Mg^{2+} ions to the solution[24, 26]. While in pure DNA solution the frequency is detected at 1079 cm^{-1}, in 0.98 mM L^{-1} Mg^{2+} ions solution the frequency downshifts to 1075 cm^{-1}, and by increasing of the Mg^{2+} concentration up to 8.33 mM L^{-1} Mg^{2+} the frequency shifts further to 1063 cm^{-1} [24]. The observed moderate frequency downshift has been interpreted as an indication of the formation of Mg^{2+}-O(H_2O)-PO_4^- aggregates, in which the water molecules solvating Mg^{2+} ion have increased acidity. This increase results in a stronger hydrogen bond between them and the phosphate groups of the DNA leading to slight decrease of the vibrational frequency of the phosphate groups. Therefore, the authors concluded that the predominant part of Mg^{2+} ions in solution do not bind directly to the phosphate groups of the nucleic acid, but rather the magnesium - phosphate interaction is mediated by a water molecule[24]. Another reason for that is the double helix structure of DNA, which does not allow the formation of tertiary loops, suitable for fixing the Mg^{2+} ions.

Magnesium and calcium ions are especially important for the functioning of chromosomal DNA[6, 7]. This is another reason to study and compare the behavior of both metals. The interaction of Ca^{2+} with the phosphate groups of DNA has been investigated via IR spectroscopy[22]. It has been shown that the peak for antisymmetric vibrations, which in absence of calcium ions is observed at 1222 cm^{-1}, splits into three peaks at 1216, 1231 and 1250 cm^{-1} after addition of Ca^{2+} ions in the solution. Increase of the peak intensity by about 30% is also observed. The results are interpreted as indication for direct interaction between the Ca^{2+} cations and the phosphate groups of DNA[22]. The different behavior of Mg^{2+} ions (solvated) and Ca^{2+} ions (bonded) can be explained by the higher ionic radius of Ca^{2+}. It allows Ca^{2+} to make more contacts at longer distances, both direct and through water molecules, with the electronegative centers of DNA. Mg^{2+}-O(PO_4^-), Ca^{2+}-O(PO_4^-) and the corresponding distances to other electronegative centers are discussed in Section 2.1. Calcium has higher electropositivity as well, thus higher affinity for the phosphate groups. XRD studies also confirm calcium ions in direct contact with the phosphate groups of double-stranded DNA. Such examples are Ca^{2+} 103 and Ca^{2+} 104 from PDB 463D[85].

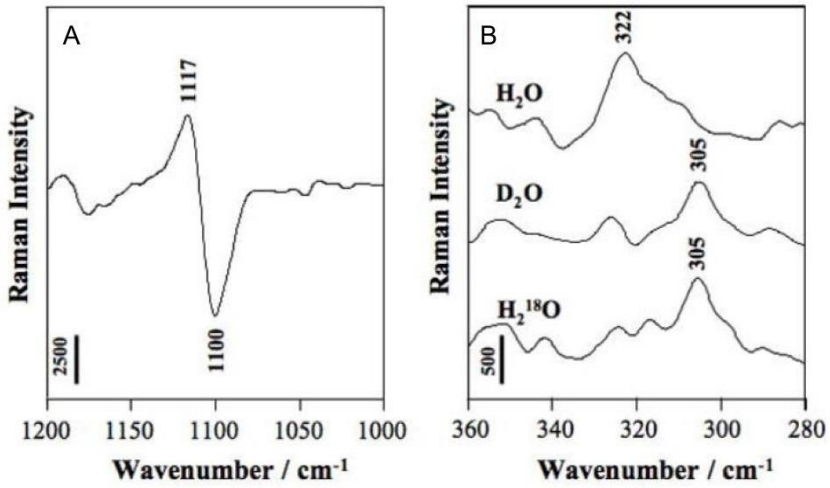

Figure 9. Raman spectra showing the difference between the Raman spectra of HDV ribozyme crystal in contact with Mg^{2+} ions (a) symmetric vibrations of the phosphate groups directly linked to Mg^{2+} ions at 1117 cm^{-1}, the negative band at 1100 cm^{-1} is due to decrease of the intensity of free phosphate groups; (b) Raman spectra indicating the presence of Mg hydrates (tetra- or pentahydrates) bound directly to phosphate groups in solution of H_2O and isotopically exchanged D_2O and $H_2{}^{18}O$ [27]. (Reprinted with permission from Ref. 27, Copyright 2008 American Chemical Society)

In contrast to the double-stranded DNA, where magnesium ions interact with phosphates via water molecules, Raman spectroscopy studies suggest that in RNA, Mg^{2+} ions are likely directly bound to the phosphate groups[27-29]. The measurements have been carried out in crystal phase. It has been shown that the symmetric vibrations of the PO_4^- groups, detected at 1100 cm^{-1} (negative band in Figure 9a), increase frequency by 17 cm^{-1} to 1117 cm^{-1} (positive band at Figure 9a). For this measurement, the RNA crystals of *Hepatitis D virus* (HDV) ribozyme have been placed in 20 mM L^{-1} solution of Mg^{2+} ions.

Another change detected in the difference spectra in Figure 9b is the positive peak at 322 cm^{-1}, assigned to metal-oxygen Mg^{2+}-O(PO_4^-) vibration in the cases when the Mg^{2+} ion is coordinated to less than six water molecules. The peak shifts from 360 cm^{-1} for magnesium hexahydrate to 322 cm^{-1} for the inner coordinated species. The isotopic change of H_2O by D_2O or $H_2{}^{18}O$ resulted in the shift of the peak at 322 cm^{-1} to 305 cm^{-1} (Figure 9b), which suggest that the peak does not involve contribution of O-H vibration since in the latter case much higher shift is expected. Thus, based on the spectra shown in Figure 9a and b, the authors concluded that there is direct interaction between the Mg^{2+} ions and the phosphate groups of RNA in the case of the HDV ribozyme[27-29].

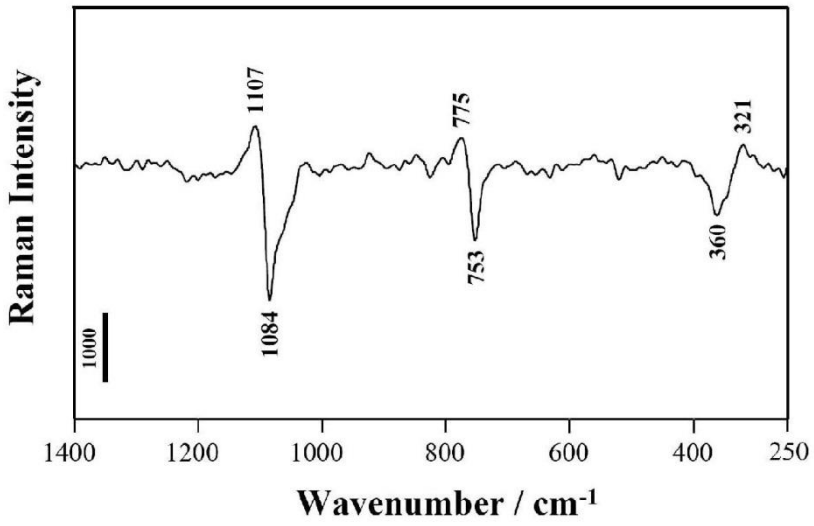

Figure 10. Raman difference spectroscopy showing the spectrum difference between 200 mM dimethyl phosphate + 1M $MgCl_2$ and 200 mM dimethyl phosphate. The background spectrum of 1M $MgCl_2$ is also subtracted in order to account for the spectrum interference of $Mg^{2+}(H_2O)_6$ [27]. (Reprinted with permission from Ref. 27, Copyright 2008 American Chemical Society)

A reference study of dimethyl phosphate solution in the presence and absence of magnesium ions in higher concentration, 1 M solution of $MgCl_2$ (Figure 10) has shown shift of three peaks related to vibration of the PO_4^- [27]. The bands at 1084, 753 and 360 cm^{-1} shift to 1107, 775 and 321 cm^{-1}. These results are interpreted as indications for direct binding of the magnesium ion to the phosphate groups, confirming the conclusions for such type of binding for RNA in HDV ribozyme. Crystallographic XRD evaluation of the HDV ribozyme structure also detects five direct bonds of the phosphate groups with Mg^{2+}. The measured distances Mg^{2+}-$O(PO_4^-)$ are less than 280 pm[86]. In addition, magnesium cations interact with the N7G and O6G atoms of the nucleobase guanine.

3.2. NMR spectroscopy

NMR spectroscopy is not among the main methods for investigation of the interaction between nucleic acids and metal ions since it can provide only indirect information about the location and dynamics of the ions. NMR studies have shown that the main part of the monovalent ions, Na^+ and K^+, remain completely solvated by water molecules in the presence of single or double-stranded DNA[5]. These ions form the so called "ion atmosphere" around the double-stranded NA. Furthermore, the NMR studies have shown that the Mg^{2+} ions prefer to bind to the major groove of NA, as well as at the stacked pair guanine-adenine bases[20]. In addition, the contacts of Mg^{2+} ions with O6 atoms of guanine have been suggested.

4. Investigation of metal ions in nucleic acids by computational methods

As described in the Introduction, the location of metal ions obtained by the X-ray crystallography cannot be applied directly to understanding their properties in the biological systems since the structure and solvation of the studied macromolecules and ions in crystal phase can differ from that in solution. The vibrational spectroscopic studies can be performed in appropriate solution but the obtained information about the location of the ions is only qualitative. Geometrical parameters like distances and angles cannot be obtained. In addition, X-ray crystallographic methods provide information about the location of the ions in a constant periodical crystal structure, whereas the results from vibrational spectroscopy approaches are characteristic for local interactions averaged for the duration of the measurement. It is essentially not possible by those approaches to follow the ion dynamic in real time in a system under conditions close to biological ones. Therefore, computational methods including both molecular dynamics approaches and isolated models have been applied to study the interaction between metal ions and nucleic acids including both local interactions and dynamics of the systems[40, 41, 87, 101].

4.1. Classical molecular dynamics simulations

The most widely used force fields for molecular dynamics of RNA systems are CHARMM and AMBER[88]. CHARMM is parameterized upon the assumption that interactions between biomolecules can be described using the MP2 *ab initio* method. The parameters, especially suitable for RNA were released in 2011 as CHARMM-36[89]. Also, it has been suggested that a degree of polarizability can be used to simulate the response of atoms to their local environment. This way a general purpose CHARMM force field is combined with a Drude harmonic oscillator. A Drude-DNA model has been found to describe better the ion–DNA interactions[90].

AMBER is amongst the most popular force fields in the area of molecule dynamics. AMBER ff99/94 are generally used, but they are not specifically designed to treats RNA. Series of improvements, specific for RNA systems have been developed, including ff99-χ_{YIL}[91], ff99-χ_{OL}[92] and the Chen and Garcia force field[93]. High-level quantum mechanical reference data and comparison with experimental results are used for their parameterization.

In the MD simulations, water models are important for the accurate estimation of solvent interaction with ions and biomolecules. Three, four and five point water models have been developed. The 3-point models include SPC/E[94] and TIP3P[95]. The more recent 4-point models include TIP4P and TIP4P-Ew[96]. Five point models were also developed, TIP5P[97]. Four point and five point models generally achieve better accuracy, at additional computational cost.

The interaction of Mg^{2+} ions with double-stranded DNA has been modeled by classical molecular dynamics (MD) simulations using AMBER ff98 force field[98]. Part of the Mg^{2+} ions was found to interact with electronegative centers of the nucleobases such as N7G and N7A nitrogen atoms of guanine and adenine as well as O6G oxygen atom of guanine. Another part

of the Mg^{2+} ions compensates the negatively charged phosphate groups of DNA[98]. The average distances to the different electronegative centers are Mg^{2+}-O6G about 400 pm; Mg^{2+}-N7G about 500 pm; Mg^{2+}-N7A about 500 pm and Mg^{2+}-PO_4^- about 800 pm. The distances of 300 to 600 pm correspond to an interaction via one or two water molecules, whereas the greater distances indicate an interaction via more than two water molecules. The data derived from the MD simulations are consistent with the conclusions from the experimental studied of DNA by vibrational spectroscopy, discussed above, that the interaction between Mg^{2+} ions and the phosphate groups is accomplished via water molecules[24, 26].

Na^+ ions are also used as counter ions in MD simulations of nucleic acids[40, 41, 87]. The interaction of double-stranded DNA with Na^+ ions has been studied, using the AMBER software package and the force field of Cornell at al. [99]. It has been found, that Na^+ ions have high affinity to the electronegative centers of the nucleobases, especially thymine and guanine[40, 41]. A direct coordination of the Na^+ ions to the carbonyl oxygen atom of thymine was observed. Part of the Na^+ ions is coordinated to the O4' oxygen atoms of deoxyribose, too. The coordination position, located in the minor groove of double-stranded DNA, was found occupied for more than 6000 ps of the simulation. Sodium ions interact with the phosphate groups of the DNA backbone either directly, or indirectly via water molecules[40, 41]. When Na^+ is coordinated to each phosphate group in the minor groove, the width of the minor groove is around 400 pm, while in absence of sodium ions, the width of the minor groove increases to around 550 pm.

Using the AMBER suite of programs with parmbsc0 modifications to the parm99 force field, Lavery *et al*. simulated the distribution of K^+ ions in DNA[100]. The study shows that highest K^+ concentration occurs within the DNA grooves, close to electronegative base sites, rather than close to the charged phosphate groups.

The interaction of metal ions with RNA is more complex than the interaction with DNA. The reason for this is the more complex tertiary and quaternary structure of RNA. The ribozyme of the *Hepatitis D virus* (HDV) is a commonly used model for studying the interaction of RNA with Na^+ and Mg^{2+} ions. MD simulations using this rybozyme have been performed with the AMBER software package and the force field Parm 99[101]. In these simulations, both fully solvated as well as directly bound Mg^{2+} ions were observed. The Mg^{2+} ions in fully hydrated state have octahedral coordination shell made up of six water molecules. During the direct interaction with electronegative centers of nucleobases, ribose or phosphate groups, the octahedral surrounding of the ion is preserved. Oxygen or nitrogen atom from the different RNA fragment takes place of a water molecule. A direct bond between Mg^{2+} and O4U oxygen atom of uracil has a length of about 198 pm, while the bond between Mg^{2+} and an oxygen atom from a phosphate group is found to be shorter, about 187 pm. It was also reported that during the simulations with total duration of 15 ns, Mg^{2+} ions do not exchange water molecules from their first coordination shells. The average life time of a water molecule from the second

solvation shell of Mg^{2+} is about 15 ps. Mg^{2+} ions were also found within the catalytic center of the HDV ribozyme[101]. There, a Mg^{2+} ion is directly bound to an oxygen atom of the phosphate group of the nucleotide U23, with a Mg^{2+}-O(PO_4^-) distance of about 185 pm and remains coordinated to 5 water molecules. One of these water molecules forms a hydrogen bond with the O2U atom of uracil (nucleotide U20). The equatorially coordinated water molecules in the surrounding of Mg^{2+} form hydrogen bonds with the phosphate groups of neighboring nucleotides G1, C22 and U23.

The water molecules from the solvation shells of Na^+ ions are much more mobile than those of Mg^{2+} shells[101]. The average lifetime of a water molecule from the first solvation shell of a fully hydrated Na^+ is 17 ps. The longest recorded duration of a water molecule in from the first solvation shell of Na^+ is 200 ps. When solvated Na^+ ions are located in the active center of the HDV ribozyme, their average resident time is 180 ps, and the maximal one is 4.3 ns. The general conclusion from the simulations is that the Na^+ ions are much more mobile than the Mg^{2+}. Sodium ions can freely migrate from the electronegative centers of RNA to the solution or from one center to another with the longest recorded duration of bound state being in the order of 6-13 ns[101].

The reason for the experimentally observed magnesium affinity for the phosphate group of RNA, see Table 1 and 5, is revealed by the use of molecular dynamics[102, 103]. Systems with directly bonded Mg^{2+} ions are fond to be much more thermodynamically stable, with much lower Gibbs free energy, compared to the cases, where the Mg^{2+} ions interact with the nitrogen bases and sugar moieties.

4.2. Quantum chemical studies using isolated models

The essential advantage of classical MD methods is that they provide the opportunity to study large scale systems and to achieve long simulation times. However, these methods also have several disadvantages. The type and strength of interactions in classical MD methods are predetermined by the used force field. Classical MD might yield incorrect results for the system/interactions if the parameterizations are inappropriate. In order to obtain results independent on the predefined parameters, the modeling should be performed with quantum chemical methods. Those methods, however, require significantly more computational resources than classical methods. Thus, the methods based on quantum chemistry are commonly applied to models or fragments with a limited number of atoms, usually in the range 50-100 atoms, which represent the most important feature of the studied system.

Model complexes of dimethyl phosphate with hydrated Mg^{2+} and Ca^{2+} ions have been studied using density functional theory approach with the hybrid exchange-correlation functional B3LYP and basis set 6-31G(d,p)[104]. The solvent (water), in which the processes presumably take place, is accounted for by the conductor-like polarizable continuum model (CPCM). The metal ion is modeled to be fully solvated as well as directly bonded to the

phosphate groups. The interaction energy has been calculated for a replacement reaction involving 1 or 2 ligands by using the following equation:

$M^{2+}(H_2O)_6 + DMP^- \rightarrow M^{2+}(H_2O)_{6-n}DMP^- + nH_2O$

where n = 0, 1 and 2 represents the ion (Mg^{2+} or Ca^{2+}) solvated by 6, 5 or 4 water molecules. The most stable complexes are those in which the Mg^{2+} ions are fully solvated. Complexes, in which the Mg^{2+} ion interacts directly with one of the O atoms of the PO_4^- group, are less stable by 48 kJ/mol. The complexes with the lowest stability (by about 100 kJ/mol lower than that of complexes containing fully solvated ions) are those in which the Mg^{2+} is in contact with two O atoms of the phosphate group and is solvated by 4 water molecules. The geometry optimization of a system with Ca^{2+}, in which the ion is fully solvated, results a Ca^{2+} directly bonded to oxygen center from PO_4^- group[104]. The complex of Ca^{2+}, in which the ion is coordinated to one O atom of PO_4^-, is found more stable by 55 kJ/mol than the case, where Ca^{2+} is coordinated to two oxygen centers of the same phosphate group[104].

Systems with Na^+, Mg^{2+} and Ca^{2+} ions directly bonded to two phosphate groups of nucleic acids have been modeled with the same simulation method and a larger basis set, 6-311++G(d,p), [46]. The cluster models used in the simulations are composed of two phosphate groups linked to the 3‘ and 5‘ hydroxyl groups of ribose or deoxyribose. The binding energy of the hydrated ions to the dinucleotide cluster models, presented in Table 6, is calculated for the following formula:

$M^{2+}(H_2O)_6 + RNA^{2-} \rightarrow RNA^{2-}M^{2+}(H_2O)_4 + 2H_2O$ (for $Na^+ = M^+$).

Table 6. Binding energies of hydrated cations to dinucleotides (in kJ/mol)[104]. Notations RNA and DNA denote that the cluster model include ribose and deoxyribose, respectively.

Complex	**Water (CPCM)**
$RNA^{2-}Mg^{2+}(H_2O)_4$	-133.5
$DNA^{2-}Mg^{2+}(H_2O)_4$	-85.4
$RNA^{2-}Ca^{2+}(H_2O)_4$	-89.9
$DNA^{2-}Ca^{2+}(H_2O)_4$	-69.0
$RNA^{2-}Na^{+}(H_2O)_4$	-17.1
$DNA^{2-}Na^{+}(H_2O)_4$	25.5

The affinity of the metal ions for binding to the phosphate groups decreases in the order $Mg^{2+} > Ca^{2+} > Na^+$, i.e. it is the highest for Mg^{2+} with binding energy of -134 kJ/mol and -85 kJ/mol for RNA and DNA models. The binding of the metal ions in the models containing ribose is stronger than those containing deoxyribose. The difference in the binding energy is about 50 kJ/mol for the complexes of Mg^{2+}, 20 kJ/mol for the complexes of Ca^{2+} and 40 kJ/mol for the complexes of Na^+, as in the latter case the positive value is calculated.

The symmetric vibrational frequency ν_s of the phosphate group is characteristic of the presence of directly bonded metal ions, as discussed above. For this reason, such frequencies have been calculated for the interaction of Mg^{2+} and Ca^{2+} ions with dimethylphosphate as a model compound[104]. The calculations are carried out with a hybrid exchange-correlation functional B3LYP and basis set 6-31G(d,p). The complexes are studied in the gas phase and by explicitly taking into account part of the solvent molecules (4 to 6 molecules of water) using the CPCM solvent model. Three cases are modeled: the metal ion is fully solvated with six water molecules and interacts with the phosphate group via water molecule (case I); the metal ion is directly bonded to one O atom of PO_4^- group and is solvated by five water molecules (case II); the metal ion is bonded to two oxygen centers from the PO_4^- fragment and is solvated by 4 water molecules (case III).

Table 7. Calculated vibrational frequencies (in cm^{-1}) of the complexes of Mg^{2+} and Ca^{2+} with dimethyl phosphate[104]. The frequencies for the complexes with Mg^{2+} and Ca^{2+} are given in the first columns. In the following columns, numerical values of the displacement for the respective complex types and conformation of PO_4^- are given. I-III corresponds to the case whether the metal ion is fully solvated, or bonded to one or two oxygen centers from a PO_4^- fragment. The letter "a" means - calculated in gas phase and "b" – calculated using polarized continuum (CPCM).

Complex	**Mg^{2+}**	**Complex**	**Mg^{2+}**	**Ca^{2+}**	**Complex**	**Mg^{2+}**	**Ca^{2+}**
I (gg)a	1027	II (gg)a	+68	1065	III (gg)a	+71	+25
I (gg)b	1057	II (gg)b	+9	1063	III (gg)b	+27	+17
I (tg)a	1071	II (tg)a	-14	1065	III (tg)a	+1	+8
I (tg)b	1058	II (tg)b	+9	1061	III (tg)b	+11	+10

Since the vibrational frequencies of PO_4^- group are affected by the conformation of fragment O=P-O-C, two conformations denoted gg and tg have been considered[104]. The terms t and g denote two possible positions of the methyl group with respect to the oxygen atoms of the phosphate group: t - trans, g - gauche. Accordingly, in gg both methyl groups are in the gauche conformation, and in tg conformation one group is trans and the other is gauche. The calculated values for the symmetric vibrations ν_s are presented in Table 7. The band shifts to higher frequencies when Mg^{2+} is directly bonded to one O atom of the phosphate group. Further shift to higher frequencies is observed when the metal ion is directly bonded to two of the O atoms. This effect is stronger in the gg conformation of the phosphate groups (Table 7). Analogous effect is also observed in the complexes of the calcium ions. Complexes of Ca^{2+}, in which the ions interact with phosphate groups through water molecules, are not modeled[104].

Sushko *et al*. reported the use of classical density functional theory (cDFT) to simulate the equilibrium ion-DNA, ion-water, and ion-ion interactions in different ionic atmospheres[105]. The simulations presented in their paper have the following model set-up: a B-form DNA molecule surrounded by an ionic atmosphere of either RbCl, $SrCl_2$, or $CoHexCl_3$ (cobalt hexammine chloride). The accuracy of the cDFT calculations was verified by comparison between experimental and simulated anomalous small-angle X-ray scattering curves. The calculations showed that there are significant differences between monovalent, divalent, and trivalent cation distributions around the B-form DNA molecule. In terms of DNA-bound Rb^+ ions: approx. 50% of them penetrate into the minor DNA groove and the other half adsorb on the backbone of the DNA molecule. As for the larger Sr^{2+} ions, their fraction in the minor groove is lower than that of Rb^+ ions, whereas all $CoHex^{3+}$ ions are adsorbed on the DNA backbone.

In addition to simulating ion-DNA interactions, quantum mechanical/molecular mechanical (QM/MM) calculations have also been used to model reaction paths in the active site of enzymes. A prominent example is the modeling of pyrophosphorolysis (i.e. reverse reaction of DNA synthesis) done by Perera *et al*. [106]. Based on their calculations, Perera *et al*. described a time-specific order of metal binding during the pyrophosphorolysis reaction. There are 3 distinct metal ion sites (the catalytic metal ion site, the nucleotide metal ion site and the product-associated metal ion site), which modulate the equilibrium of the above-cited biochemical process. However, a specific set of sodium and magnesium ions must occupy the 3 distinct metal ion sites so that the reaction can occur. According to the reported QM/MM calculation results, pyrophosphorolysis is initiated when the catalytic metal site is occupied by a magnesium ion. The nucleotide metal ion site is occupied by a magnesium ion throughout the whole reaction. In contrast, the product metal site is occupied by a magnesium ion only in the early stages of the reaction. In the later stages of the reaction, a magnesium ion in the product metal site acts as a reaction inhibitor, and hence is replaced by a sodium ion.

Replica-exchange molecular dynamics (REMD) is another method, used to study metal ions affecting the function of biomolecules. Swadling *et al*. investigated how structure and dynamics influence the function of a ribozyme in different inorganic settings. The full hammerhead ribozyme is used as a model[107]. It was discovered, by sampling major conformational states, that its structure can manifest a free-energy landscape similar to that of proteins which have a “funnel” topology. The analysis of the ribozyme’s conformations explains the experimentally observed differences between the catalytic activity in bulk water and when it interacts with clay materials.

4.3. *Ab initio* molecular dynamic simulations

A study of the interactions between sodium and magnesium ions and the RNA phosphate groups, in water solution, is performed using *ab initio* Born – Oppenheimer molecular

dynamics. Duration of the simulations is about 140 ps. Results analysis has shown that sodium ions are notably more mobile than the Mg^{2+} (Figure 11)[49] . Each type of the modeled ions can be either directly bonded to the phosphate group or completely solvated by water molecules.

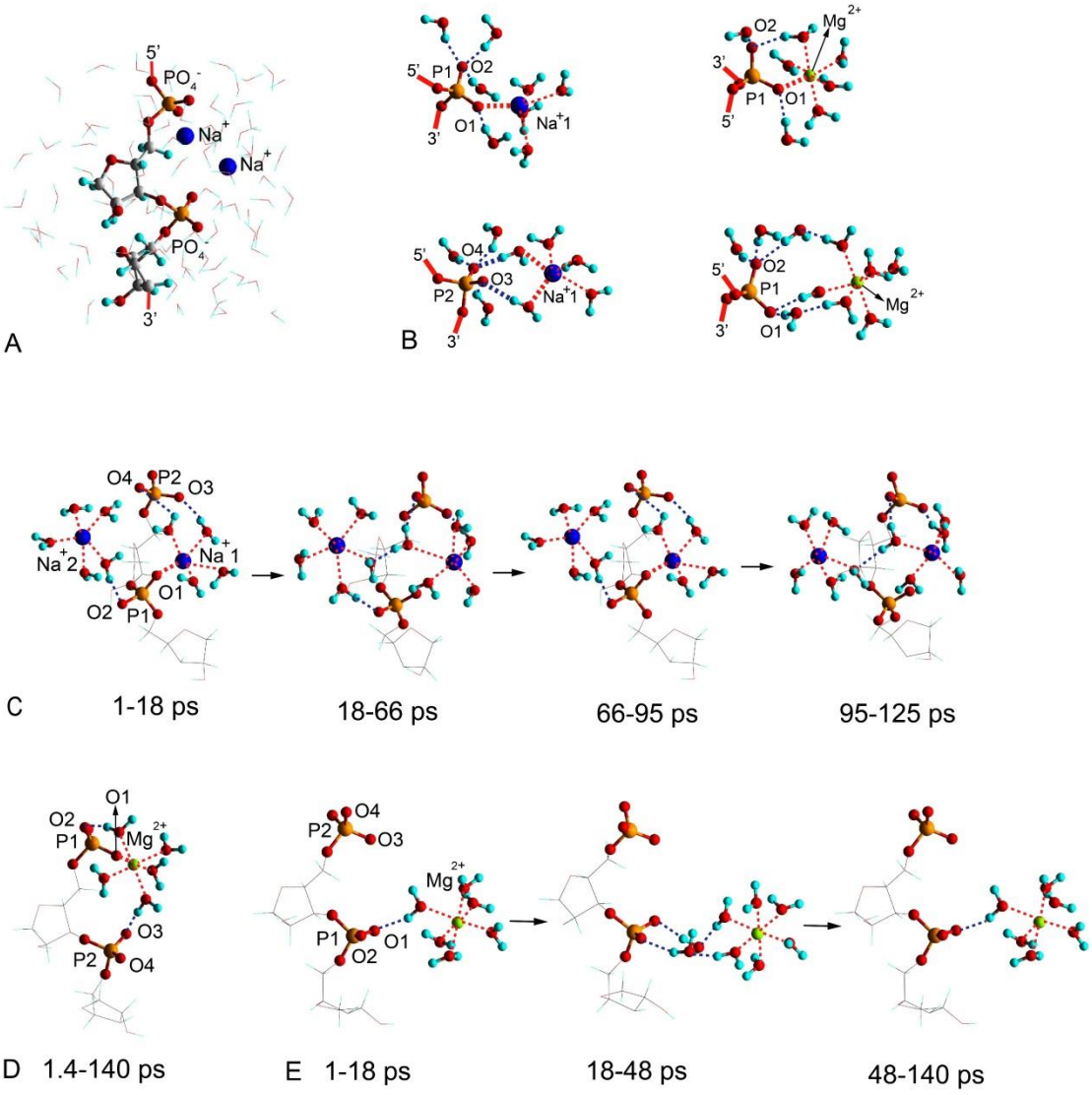

Figure 11. Selected moments from the simulation: (a) the periodic box in which the simulation was carried out containing a phosphate backbone of RNA and two sodium ions (water molecules are simply depicted as lines); (b) the water molecules solvating the phosphate groups P1 and P2 as well as the cations in directly bonded or completely solvated state; (c) the sodium ions in different moments of the simulation; (d) the directly bonded magnesium ion and (e) the completely solvated magnesium ion in different moments of the simulation. (Reprinted with permission from Ref. 49, Copyright 2013 American Chemical Society)

Sodium ion changes its position between coordinated to the phosphate group at about 235 pm, and completely solvated by water. During the simulation, the ion remains directly bonded to the phosphate for approximately 20-30 ps, e.g. 20 % of the time. The sodium ions can coordinate from 4 to 7 oxygen atoms from water molecules or phosphate groups in their first coordination shell with the most frequent coordination number being 5 (approx. 80% of simulation time), followed by 6 (approx. 15% of simulation time).

In the system with two sodium ions, the potential energy local minima and maxima do not correlate to some specific positions of the metal ions in respect to the phosphate groups. Potential energy fluctuations indicate variations in the arrangement of water molecules in the system. The average value of the potential energy, when the ion Na^+ is directly bonded, is lower than the case, when the ion is completely solvated, by 6 kJ/mol. This value is negligibly small for the system. Similarly, the local minima and maxima of the systems with Mg^{2+} do not correlate to some specific positions of the ions in relation to the phosphate groups.

During the entire simulations, the magnesium ions do not change their initial position - they remain directly bonded to the phosphate group or completely solvated. The magnesium ion binds to one of the oxygen atoms of the phosphate group with an optimal distance of 205 pm.

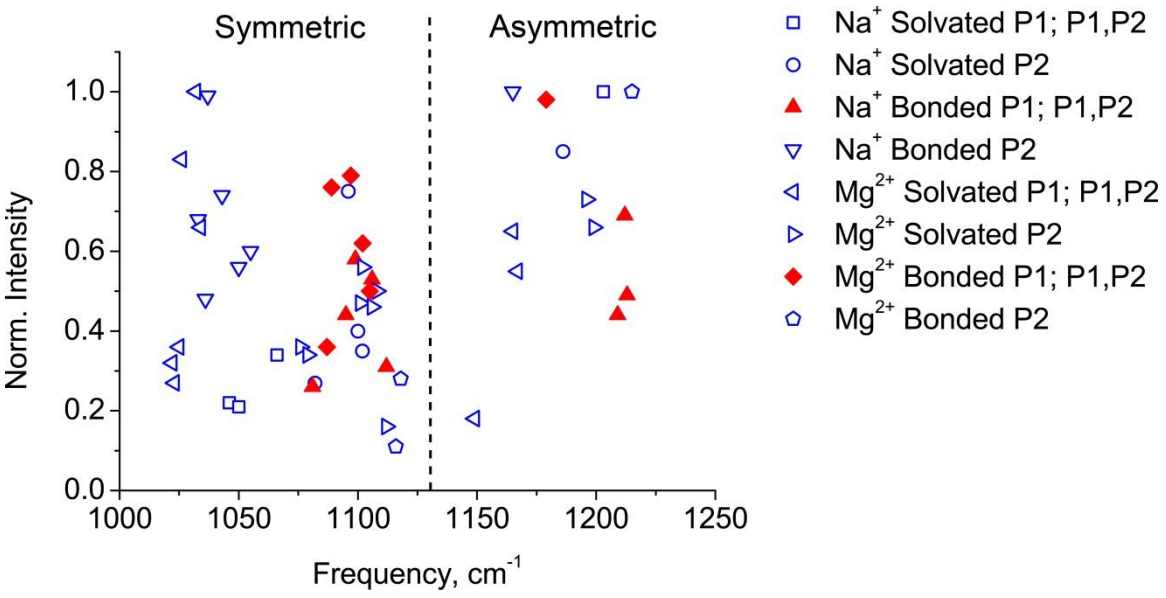

Figure 12. Calculated frequencies of the symmetric and asymmetric vibrations of the phosphate groups and their normalized intensities. The filled red symbols indicate vibrations of a phosphate group which has a bonded metal ion. The empty blue symbols indicate vibrations of a phosphate group which is solvated only by water molecules with no metal ion bonded. (Reprinted with permission from Ref. 49, Copyright 2013 American Chemical Society)

A complete vibration analysis, explicitly including water molecules, shows that the symmetrical vibrations of the phosphate groups can be used to determine the position of the sodium or magnesium ion with respect to the phosphate groups. In the absence of a directly bonded cation, both a low frequency as well as a high frequency zones are observed. If a directly bonded cation is presented, the intensity of the low frequency vibrations decreases and that of the high frequency vibrations increases, Figure 12. Note that P1 and P2 indicate the different phosphate groups in the model. When the metal ion is directly bonded, it is attached to the P1 group. Experimental Raman spectroscopy results confirm the shifting to higher frequencies, when directly bonded cation is presented[27].

5. Summary and outlook

Alkaline and alkaline earth metal ions play an important role for the stability and formation of tertiary and quaternary structures of different types of nucleic acids, in particular RNA and the ribosome. Magnesium ions are critical for preserving the tertiary structure of RNA. Their presence, especially between phosphate groups, stabilizes the folding of the molecule. Negatively charged groups are bridged, thus transforming electrostatic repulsion between them into attraction. Quaternary structure of the ribosome also depends on the presence of Mg^{2+} ions, as they contribute to the coupling of the small and large subunits. Tertiary ribosomal structure and in particular the structure of the peptidyl transferase center are stabilized by Na^{+}, K^{+} and Mg^{2+} ions. This stabilization is achieved by non-specific compensation of the phosphate groups' negative charges (especially by K^{+} ions) and by coordination of the cation to specific centers (the most typical for Mg^{2+} ions). Thus, those cations are needed for the ribosome to perform its function (peptide synthesis) without participating directly in the catalytic process.

All cations, considered in the present review, Na^{+}, K^{+}, Mg^{2+} and Ca^{2+}, are required for the maintaining of chromosomal DNA structural integrity. They perform this function mainly by neutralization of the phosphate groups' negative charges. Mg^{2+} and Ca^{2+} are especially important, because they can bridge distant phosphate groups, and additionally contribute for the packing of DNA. Ca^{2+} ions are more probable to bridge the groups by direct contacts. Mg^{2+} ions can perform this task either by binding to the phosphate groups directly or via water molecules.

As described above, the crystallographic methods and various spectroscopies, IR, Raman, and NMR, are used to study the static interactions between ions and nucleic acids, mainly in crystal phase. Those methods suggest that divalent ions can be bonded directly or indirectly to more than one phosphate group or other electronegative centers, thus forming a bridge between different parts of the macromolecules or between different macromolecules. The monovalent cations with their specific ionic radii and affinity for water molecules and the nitrogen centers from the electronegative bases can stabilize quadruplex structures. The

monovalent cations bonded to the nitrogen bases interact with the phosphate groups usually through one or two water molecules forming ionic atmosphere around the nucleic acids.

Computational methods provide the means to study the affinity and dynamics of monovalent and divalent ions around DNA and RNA at an atomic scale. Classical methods suggest that divalent cations bind to specific centers of RNA, containing phosphate groups, and in this bonded state they can remain for a time in the order of nanoseconds or more. In particular, magnesium ions do not exchange water molecules of their first coordination shells for a time of about 15 ns. Both classical and ab initio simulations suggest that the monovalent cations generally have picosecond dynamics and often change their position towards the RNA nucleotides and that the water molecules of their first solvation shell are much more mobile.

The combination of experimental and theoretical methods suggests that divalent cations, Mg^{2+} and Ca^{2+}, have high affinity to the phosphate groups of the nucleic acids. On the other hand, Na^{+} and K^{+} have higher affinity to the nitrogen bases and are often found in the groves of RNA or DNA. Also, the monovalent ions are much more mobile than the divalent ones. Thus, the combination of experimental and theoretical methods is the most productive strategy for the study of metal ions-nucleic acids interactions. This is essential if an atomic scale resolution is needed in a dynamic environment.

Conflicts of interest

There are no conflicts of interest to declare.

Acknowledgments

PStP and GNV are grateful for the support by the Horizon2020 program of the European Commission (project Materials Networking - grant agreement 692146).

References

1 D. Celander and T. Cech, Visualizing the higher order folding of a catalytic RNA molecule, *Science*, 1991, **251**, 401-407.

2 A. Sigel, H. Sigel and R. Sigel, *Structural and catalytic roles of metal ions in RNA*, RSC Publishing, Cambridge UK, 2011.

3 M. Serra, J. Baird, T. Dale, B. Fey, K. Retatagos and E. Westhof, Effects of magnesium ions on the stabilization of RNA oligomers of defined structures, *RNA*, 2002, **8**, 307-323.

4 P. Auffinger, L D'Ascenzo and E. Ennifar, in *The Alkali Metal Ions: Their Role for Life*, ed. A. Sigel, H. Sigel and R. K. O. Sigel, Springer, 2016, Sodium and potassium interactions with nucleic acids, 167-203.

5 D. E. Draper, A guide to ions and RNA structure, *RNA*, 2004, **10**, 335-343.

6 R. Strick, P. L. Strissel, K. Gavrilov and R. Levi-Setti, Cation–chromatin binding as shown by ion microscopy is essential for the structural integrity of chromosomes, *J. Cell Biol.*, 2001, **55**, 899-910.

7 R. Levi-Setti, K. L. Gavrilov and P. J. Rizzo, Divalent cation distribution in dinoflagellate chromosomes imaged by high-resolution ion probe mass spectrometry, *Eur. J. Cell Biol.*, 2008, **87**, 963-976.

8 N. V. Hud and M. Polak, DNA–cation interactions: the major and minor grooves are flexible ionophores, *Curr. Opin. Struct. Biol.*, 2001, **11,** 293-301.

9 M. Egli, DNA-cation interactions: Quo vadis?, *Chem. Biol.*, 2002, **9,** 277-286.

10 S. J. Chen, RNA folding: conformational statistics, folding kinetics, and ion electrostatics, *Annu. Rev. Biophys.*, 2008, **37**, 197-214.

11 D. J. Klein, P. B. Moore and T. A. Steitz, The contribution of metal ions to the structural stability of the large ribosomal subunit, *RNA*, 2004, **10**, 1366-1379.

12 A. Bashan and A. J. Yonath, The linkage between ribosomal crystallography, metal ions, heteropolytungstates and functional flexibility, *J. Mol. Struct.*, 2008, **890**, 289-294.

13 S. A. Strobel and J. C. Cochrane, RNA catalysis: ribozymes, ribosomes, and riboswitches, *Curr. Opin. Chem. Biol.*, 2007, **11**, 636-643.

14 S. Shan, A. V. Kravchuk, J. A. Piccirilli and D. Herschlag, Defining the catalytic metal ion interactions in the Tetrahymena ribosome reaction, *Biochemistry*, 2001, **40**, 5161-5171.

15 F. Guo, A. R. Gooding and T. R. Cech, Structure of the Tetrahymena ribozyme: base triple sandwich and metal ion at the active site, *Mol. Cell*, 2004, **16**, 351-362.

16 F. Leclerc, Hammerhead ribozymes: true metal or nucleobase catalysis? Where is the catalytic power from?, *Molecules*, 2010, **15**, 5389-5407.

17 A. Garcia-Sacristán, M. Moreno, A. Ariza-Mateous, E. López-Camacho, R. M. Jáudenes, L. Vázquez, J. Gómez, J. Á. Martín-Gago and C. Briones, A magnesium-induced RNA conformational switch at the internal ribosome entry site of hepatitis C virus genome visualized by atomic force microscopy, *Nucleic Acids Res.*, 2015, **43**, 565–580.

18 K. Mizoguchi, Electronic states of M-DNA incorporated with divalent metal ions, *Nanobiosystems: Processing, Characterization, and Applications III, Proc. of SPIE*, 2010, **7765**, 77650R-1.

19 S. Johannsen, N. Megger, D. Böhme, R. K. O. Sigel and J. Müller, Solution structure of a DNA double helix with consecutive metal-mediated base pairs, *Nature Chem.*, 2010, **2**, 229-234.

20 Q. Zhao, U. Nagaswamy, H. Lee, Y. Xia, H. Huang, X Gao and G. E. Fox, NMR structure and Mg^{2+} binding of an RNA segment that underlies the L7/L12 stalk in the E.coli 50S ribosomal subunit, *Nucleic Acids Res.*, 2005, **33**, 3145-3153.

21 B. Fürtig, C. Richter, J. Wöhnert and H. Schwalbe, NMR Spectroscopy of RNA, *ChemBioChem*, 2003, **4**, 936-962.

22 R. Ahmad, H. Arakawa and H. A. Tajmir-Riahi, A comparative study of DNA complexation with Mg(II) and Ca(II) in aqueous solution: major and minor grooves bindings, *Biophys. J.*, 2003, **84**, 2460-2466.

23 L. Chiriboga, P. Xie, H. Yee, V. Vigorita, D. Zarou, D. Zakim and M. Diem, Infrared spectroscopy of human tissue. I. Differentiation and maturation of epithelial cells in the human cervix, *Biospectroscopy*, 1998, **4**, 47-53.

24 S. Ponkumar, P. Duraisamy and N. Iyandurai, Structural analysis of DNA interactions with magnesium ion studied by Raman spectroscopy, *Am. J. Biochem. Biotechnol.*, 2011, **7**, 135-140.

25 J. Duguid, V. A. Bloomfield, J. Benevides and G. J. Thomas Jr., Raman spectroscopy of DNA-metal complexes. I. Interactions and conformational effects of the divalent cations: Mg, Ca, Sr, Ba, Mn, Co, Ni, Cu, Pd, and Cd, *Biophys. J.*, 1993, **65**, 1916-1928.

26 N. Iyandurai and R. Sarojini, Magnesium (II) ion induced changes on the structure of DNA: an FT–Raman study, *J. Appl. Sci. Res.*, 2009, **5**: 283-285.

27 B. Gong, Y. Chen, E. L. Christian, J. H. Chen, E. Chase, D. M. Chadalavada, R. Yajima, B. L. Golden, P. C. Bevilacqua and P. R. J. Carey, Detection of innersphere interactions between magnesium hydrate and the phosphate backbone of the HDV ribozyme using Raman crystallography, *Am. Chem. Soc.*, 2008, **130,** 9670-9672.

28 J. H. Chen, B. Gong, P. C. Bevilacqua, P. R. Carey and B. L. Golden, A catalytic metal ion interacts with the cleavage site G·U wobble in the HDV ribozyme, *Biochemistry*, 2009, **48**, 1498-1507.

29 B. Gong, J. H. Chen, R. Yajima, Y. Chen, E. Chase, D. M. Chadalavada, B. L. Golden, P. R. Carey and P. C. Bevilacqua, Raman crystallography of RNA, *Methods*, 2009, **49**, 101-111.

30 J. Stangret and R. Savoie, Vibrational spectroscopic study of the interaction of metal ions with diethyl phosphate, a model for biological systems, *Can. J. Chem.*, 1992, **70**, 2875-2883.

31 Y. Guan, C. J. Wurrey and G. J. Thomas Jr., Vibrational analysis of nucleic acids. I. The phosphodiester group in dimethyl phosphate model compounds: $(CH_3O)_2PO_2^-$, $(CD_3O)_2PO_2^-$, and $(^{13}CH_3O)_2PO_2^-$, *Biophys. J.*, 1994, **66**, 225-235.

32 P. L. Anto, R. J. Anto, H. T. Varghese, C. Y. Panicker and D. Philip, Vibrational spectroscopic studies and *ab initio* calculations of phenyl phosphate disodium salt, *J. Raman Spectrosc.*, 2010, **41**, 113-119.

33 S. M. Perepelytsya and S. N. Volkov, Intensities of DNA ion-phosphate modes in the low-frequency Raman spectra, *Eur. Phys. J. E*, 2010, **31**, 201-205.

34 E. Ennifar, P. Walter and P. Dumas, Cation-dependent cleavage of the duplex form of the subtype-B HIV-1 RNA dimerization initiation site, *Nucleic Acids Res.*, 2010, **38**, 5807-5816.

35 M. Egli, G. Minasov, L. Su and A. Rich, Metal ions and flexibility in a viral RNA pseudoknot at atomic resolution, *Proc. Natl. Acad. Sci. USA*, 2002, **99**, 4302-4307.

36 C. C. Correll, B. Freeborn, P. B. Moore and T. A. Steitz, Metals, motifs, and recognition in the crystal structure of a 5S rRNA domain, *Cell*, 1997, **91**, 705-712.

37 J. A. Subirana and M. Soler-López, Cations as hydrogen bond donors: a view of electrostatic interactions in DNA, *Annu. Rev. Biophys. Biomol. Struct.*, 2003, **32**, 27-45.

38 C. Sines, L. McFail-Isom, S. Howerton, D. VanDerveer and L. Williams, Cations mediate B-DNA conformational heterogeneity, *J. Am. Chem. Soc.*, 2000, **122**, 11048-11056.

39 P. Auffinger and E. Westhof, Water and ion binding around RNA and DNA (C, G) oligomers, *J. Mol. Biol.*, 2000, **300**, 1113-1131.

40 D. Hamelberg, L. McFail-Isom, L. Williams and W. Wilson, Flexible structure of DNA: ion dependence of minor-groove structure and dynamics, *J. Am. Chem. Soc.*, 2000, **122**, 10513-10520.

41 D. Hamelberg, L. Williams and W. Wilson, Influence of the dynamic positions of cations on the structure of the DNA minor groove: sequence-dependent effects, *J. Am. Chem. Soc.*, 2001, **123**, 7745-7755.

42 N. Korolev, A. P. Lyubartsev, A. Rupprecht and L. Nordenskiöld, Competitive binding of Mg^{2+}, Ca^{2+}, Na^{+}, and K^{+} ions to DNA in oriented DNA fibers: experimental and Monte Carlo simulation results, *Biophys. J.*, 1999, **77**, 2736-2749.

43 J. Yoo and A. Aksimentiev, Improved parametrization of Li^{+}, Na^{+}, K^{+}, and Mg^{2+} ions for all-atom molecular dynamics simulations of nucleic acid systems, *J. Phys. Chem. Lett.*, 2012, **3**, 45−50.

44 F. Ryjacek, T. Kubar and P. J. Hobza, New parameterization of the Cornell *et al*. empirical force field covering amino group nonplanarity in nucleic acid bases, *Comput. Chem.*, 2003, ***24***, 1891–1901.

45 M. Ditzler, M. Otyepka, J. Sponer and N. Walter, Molecular dynamics and quantum mechanics of RNA: conformational and chemical change we can believe in, *Acc. Chem. Res.*, 2010, **43**, 40-47.

46 A. Petrov, J. Bowman, S. Harvey and L. Williams, Bidentate RNA–magnesium clamps: on the origin of the special role of magnesium in RNA folding, *RNA*, 2011, **17**, 291-297.

47 P. Banas, P. Jurecka, N. G. Walter, J. Sponer and M. Otyepka, Theoretical studies of RNA catalysis: hybrid QM/MM methods and their comparison with MD and QM, *Methods*, 2009, **49**, 202-216.

48 D. Di Tommaso and N. H. De Leeuw, Structure and dynamics of the hydrated magnesium ion and of the solvated magnesium carbonates: insights from first principles simulations, *Phys. Chem. Chem. Phys.*, 2010, **12**, 894-901.

49 S. Kolev, P. Petkov, M. Rangelov and G. Vayssilov, *Ab initio* molecular dynamics of Na^{+} and Mg^{2+} countercations at the backbone of RNA in water solution, *ACS Chemical Biology*, 2013, **8**, 1576–1589.

50 Y. Tanaka, S. Yamagata, Y. Kitago, Y. Yamada, S. Chimnaronk, M. Yao and I. Tanaka, Deduced RNA binding mechanism of ThiI based on structural and binding analyses of a minimal RNA ligand, *RNA*, 2009, **15**, 1498-1506.

51 J. Nix, D. Sussman and C. Wilson, The 1.3 Å crystal structure of a biotin-binding pseudoknot and the basis for RNA molecular recognition, *J. Mol. Biol.*, 2000, **296**, 1235-1244.

52 J. Deng, Y. Xiong and M. Sundaralingam, X-ray analysis of an RNA tetraplex (UGGGGU) 4 with divalent Sr^{2+} ions at subatomic resolution (0.61 Å), *Proc. Natl. Acad. Sci. USA*, 2001, **98**, 13665-13670.

53 J. A. Ippolito and T. A. Steitz, A 1.3-Å resolution crystal structure of the HIV-1 trans-activation response region RNA stem reveals a metal ion-dependent bulge conformation, *Proc. Natl. Acad. Sci. USA*, 1998, **95**, 9819-9824.

54 P. S. Pallan, W. S. Marshall, J. Harp, F. C. Jewett III, Z. Wawrzak, B. A. Brown II, A. Rich and M. Egli, Crystal structure of a luteoviral RNA pseudoknot and model for a minimal ribosomal frameshifting motif, *Biochemistry*, 2005, **44**, 11315-11322.

55 E. Ennifar and P. Dumas, Polymorphism of bulged-out residues in HIV-1 RNA DIS kissing complex and structure comparison with solution studies, *J. Mol. Biol.*, 2006, **256**, 771-782.

56 U. Mueller, Y. A. Muller, R. Herbst-Irmer, M. Sprinzl and U. Heinemann, Disorder and twin refinement of RNA heptamer double helices, *Acta Crystallogr. Sect. D*, 1999, **55**, 1405-1413.

57 U. Mueller, H. Schubel, M. Sprinzl and U. Heinemann, Crystal structure of acceptor stem of tRNA Ala from Escherichia coli shows unique G.U wobble base pair at 1.16 Å resolution, *RNA*, 1999, **5**, 670-677.

58 T. Hermann, V. Tereshko, E. Skripkin and D. Patel, Apramycin recognition by the human ribosomal decoding site, *J. Blood Cells Mol. Dis.*, 2007, **38**, 193-198.

59 B. H. Mooers and A. Singh, The crystal structure of an oligo (U): pre-mRNA duplex from a trypanosome RNA editing substrate, *RNA*, 2011, **17**, 1870-1883.

60 S. Freisz, K. Lang, R. Micura, P. Dumas and E. Ennifar, Binding of aminoglycoside antibiotics to the duplex form of the HIV-1 genomic RNA dimerization initiation site, *Angew. Chem. Int. Ed. Engl.*, 2008, **47**, 4110-4113.

61 G. Storz, An expanding universe of noncoding RNAs, *Science*, 2002, **296**, 5571, 1260

62 H. Zheng, I. G. Shabalin, K. B. Handing, J. M. Bujnicki and W. Minor, Magnesium-binding architectures in RNA crystal structures: validation, binding preferences, classification and motif detection, *Nucleic Acids Res.*, 2015, **43**, 3789–3801.

63 H. Lodish, A. Berk, L. Zipursky, P. Matsudaira, D. Baltimore and J. Darnell, *Molecular cell biology, 4th edition*, W. H. Freeman, New York NY, 2000.

64 M. A. Rangelov, G. N. Vayssilov, V. M. Yomtova and D. D. Petkov, The syn-oriented 2-OH provides a favorable proton transfer geometry in 1,2-diol monoester aminolysis: implications for the ribosome mechanism, *J. Am. Chem. Soc.*, 2006, **128**, 4964–4965.

65 M. A. Rangelov, G. P. Petrova, V. M. Yomtova and G. N. Vayssilov, Catalytic role of vicinal OH in ester aminolysis: proton shuttle versus hydrogen bond stabilization, *J. Org. Chem.*, 2010, **75**, 6782–6792.

66 B. Hingerty, R. S. Brown and A. Jack, Further refinement of the structure of yeast tRNAPhe, *J. Mol. Biol.*, 1978, **124**, 523-534.

67 E. Westhof, P. Dumas and D. Moras, Restrained refinement of two crystalline forms of yeast aspartic acid and phenylalanine transfer RNA crystals, *Acta Crystallogr. Sect. A*, 1988, **44**, 112-123.

68 E. Westhof and M. Sundaralingam, Restrained refinement of the monoclinic form of yeast phenylalanine transfer RNA. Temperature factors and dynamics, coordinated waters, and base-pair propeller twist angles, *Biochemistry*, 1986, **25**, 4868-4878.

69 J. L. Sussman, S. R. Holbrook, R. W. Warrant, G. M. Church and S. H. Kim, Crystal structure of yeast phenylalanine transfer RNA: I. Crystallographic refinement, *J. Mol. Biol.*, 1978, **123**, 607-630.

70 H. Shi and P. B. Moore, The crystal structure of yeast phenylalanine tRNA at 1.93 Å resolution: a classic structure revisited, *RNA*, 2000, **6**, 1091-1105.

71 S. Basu, R. P. Rambo, J. Strauss-Soukup, J. H. Cate, A. R. Ferre-D'Amare, S. A. Strobel and J. A. Doudna, A specific monovalent metal ion integral to the AA platform of the RNA tetraloop receptor, *Nat. Struct. Biol.*, 1998, **5**, 986–992.

72 R. Shiman and D. E. Draper, Stabilization of RNA tertiary structure by monovalent cations, *J. Mol. Biol.*, 2000, **302**, 79–91.

73 F. C. Chao and H. K. Schachman, The isolation and characterization of a macromolecular ribonucleoprotein from yeast, *Arch. Biochem. Biophys.*, 1956, **61**, 220–230.

74 F. C. Chao, Dissociation of macromolecular ribonucleoprotein of yeast, *Arch. Biochem. Biophys.*, 1957, **70**, 426–431.

75 A. Tissieres, J. D. Watson, D. Schlessinger and B. R. Hollingworth, Ribonucleoprotein particles from Escherichia coli, *J. Mol. Biol.*, 1959, **1**, 221–233.

76 B. McCarthy, The effects of magnesium starvation on the ribosome content of Escherichia coli, *J. Biochim. Biophys. Acta.*, 1962, **55**, 880–888.

77 B. W. Kimes and D. R. Morris, Cations and ribosome structure. II. Effect of the 50S subunit of substituting polyamines for magnesium ion, *Biochemistry*, 1973, **12**, 442–449.

78 J. Gordon and F. Lipmann, Role of divalent ions in poly U-directed phenylalanine polymerization, *J. Mol. Biol.*, 1967, **23**, 23–33.

79 P. B. Moore, Polynucleotide attachment to ribosomes, *J. Mol. Biol.*, 1966, **18**, 8–20.

80 J. A. Khawaja and A. Raina, Effect of spermine and magnesium on the attachment of free ribosomes to endoplasmic reticulum membranes in vitro, *Biochem. Biophys. Res. Commun.*, 1970, **41**, 512–518.

81 P. H. Naslund and T. Hultin, Effects of potassium deficiency on mammalian ribosomes, *Biochim. Biophys. Acta.*, 1970, **204**, 237–247.

82 R. S. Zitomer and J. G. Flaks, Magnesium dependence and equilibrium of the Escherichia coli ribosomal subunit association, *J. Mol. Biol.*, 1972, **71**, 263–279.

83 N. Ban, P. Nissen, J. Hansen, B. Moore and A. Steitz, The complete atomic structure of the large ribosomal subunit at 2.4 A resolution, *Science*, 2000, **289**, 905-920.

84 J. H. Cate and J. A. Doudna, Metal-binding sites in the major groove of a large ribozyme domain, *Structure*, 1996, **4**, 1221-1229.

85 J. Liu and A. Subirana, Structure of d(CGCGAATTCGCG) in the presence of Ca(2+) ions, *J. Biol. Chem.*, 1999, **274**, 24749-24752.

86 A. R. Ferre-D'Amare, K. Zhou and J. A. Doudna, Crystal structure of a hepatitis delta virus ribozyme, *Nature*, 1998, **395**, 567.

87 J. Schwarz, C. Contescu and K. Putyera, *Dekker Encyclopedia of Nanoscience and Nanotechnology*, Marcel Dekker, Inc., New York, NY, 2004.

88 S. Vangaveti, S. Ranganathan and A. Chen, Advances in RNA molecular dynamics: a simulator's guide to RNA force fields, *Wiley Interdiscip. Rev. RNA*, 2017, **8**(2).

89 E. J. Denning, U. D. Priyakumar and L. Nilsson, Impact of 20-hydroxyl sampling on the conformational properties of RNA: update of the CHARMM all-atom additive force field for RNA, *J. Comput. Chem.*, 2011, **32**, 1929–1943.

90 A. Savelyev and A. D. MacKerell, All-atom polarizable force field for DNA based on the classical Drude oscillator model, *J. Comput. Chem.*, 2014, **35**, 1219–1239.

91 I. Yildirim, S. D. Kennedy, H. A. Stern, J. M. Hart, R. Kierzek and D. H. Turner, Revision of AMBER torsional parameters for RNA improves free energy predictions for tetramer duplexes with GC and iGiC base pairs, *J. Chem. Theory Comput.*, 2012, **8**, 172–181.

92 M. Zgarbova, M. Otyepka, J. Sponer, A. Mladek, P. Banas and P. Jurecka, Refinement of the Cornell *et al*. nucleic acids force field based on reference quantum chemical calculations of glycosidic torsion profiles, *J. Chem. Theory Comput.*, 2011, **7**, 2886–2902.

93 A. A. Chen and A. E. Garcia, High-resolution reversible folding of hyperstable RNA tetraloops using molecular dynamics simulations, *Proc. Natl. Acad. Sci. USA*, 2013, **110**, 16820–16825.

94 H. J. C. Berendsen, J. R. Grigera and T. P. Straatsma, The missing term in effective pair potentials, *J. Phys. Chem.*, 1987, **91**, 6269.

95 W. L. Jorgensen, J. Chandrasekhar, J. D. Madura, R. W. Impey and M. L. Klein, Comparison of simple potential functions for simulating liquid water, *J. Chem. Phys.*, 1983, **79**, 926.

96 H. W. Horn, W. C. Swope, J. W. Pitera, J. D. Madura, T. J. Dick, G. L. Hura and T. Head-Gordon, Development of an improved four-site water model for biomolecular simulations: TIP4P-Ew, *J. Chem. Phys.*, 2004, **120**, 9665–9678.

97 M. W. Mahoney and W. L. Jorgensen, A five-site model for liquid water and the reproduction of the density anomaly by rigid, nonpolarizable potential functions, *J. Chem. Phys.*, 2000, **112**, 8910.

98 M. Gueroult, O. Boittin, O. Mauffret, C. Etchebest and B. Hartmann, Mg^{2+} in the major groove modulates B-DNA structure and dynamics, *PloS one*, 2012, **7**, e41704.

99 W. D. Comell, P. Cieplak, C. I. Bayly, I. R. Gould, K. M. Merz, D. M. Ferguson, D. C. Spellmeyer, T. Fox, J. W. Caldwell and P. A. Kollman, A second generation force field for the simulation of proteins, nucleic acids, and organic molecules, *J. Am. Chem. Soc.*, 1995, **117**, 5179-5196.

100 M. Pasi, J. Maddocks and R. Lavery, Analyzing ion distributions around DNA: sequence-dependence of potassium ion distributions from microsecond molecular dynamics, *Nucleic Acids Research*, 2015, **43**, 2412–2423.

101 M. Krasovska, J. Sefcikova, K. Reblova, B. Schneider, N. G. Walter and J. Sponer, Cations and hydration in catalytic RNA: molecular dynamics of the hepatitis delta virus ribozyme, *Biophys. J.*, 2006, **91**, 626-638.

102 H. Zheng, I. G. Shabalin, K. B. Handing, J. M. Bujnicki and W. Minor, Magnesium-binding architectures in RNA crystal structures: validation, binding preferences, classification and motif detection, *Nucleic Acids Res.*, 2015, **43**, 3789–3801.

103 R. Cunha and G. Bussi, Unraveling Mg^{2+}-RNA binding with atomistic molecular dynamics, *RNA*, 2017, **23**, 628–638.

104 A. Petrov, J. Funseth-Smotzer and G. Pack, Computational study of dimethyl phosphate anion and its complexes with water, magnesium, and calcium, *Int. J. Quantum Chem.*, 2005, **102**, 645-655.

105 M. L. Sushko, D. G. Thomas, S. A. Pabit, L. Pollack, A. V. Onufriev and N. A. Baker, The role of correlation and solvation in ion interactions with B-DNA, *Biophys. J.*, 2016, **110**, 315-326.

106 L. Perera, B. D. Freudenthal, W. A. Beard, D. D. Shock, L. G. Pedersen and S. H. Wilson, Requirement for transient metal ions revealed through computational analysis for DNA polymerase going in reverse, *Proc. Natl. Acad. Sci. USA*, 2015, **112**, E5228–E5236.

107 J. B. Swadling, D. W. Wright, J. L. Suter and P. V. Coveney, Structure, dynamics, and function of the hammerhead ribozyme in bulk water and at a clay mineral surface from replica exchange molecular dynamics, *Langmuir*, 2015, **31**, 2493−2501.